December 2019

Euclidean Dynamical Triangulations: Running Couplings and Curvature Correlation Functions

Scott David Bassler
Syracuse University

Abstract

Quantum field theories have been incredibly successful at describing many fundamental aspects of reality with great precision, sometimes relying on the powerful computational tool of lattice methods. Gravity has so far eluded a quantum field theory description, leading many to consider more exotic theories like String Theory. However, recent results in lattice quantum gravity have brought some renewed interest in the subject. After reviewing the progress made so far in Euclidean Dynamical Triangulations (EDT), a lattice theory of gravity, we examine how the couplings of the theory run with scale, and discover that their runnings are consistent with the asymptotic safety scenario for gravity with a 1-dimensional UV critical surface, making it maximally predictive. We also study two-point curvature correlation functions for gravity, and upon removing the disconnected contributions, we find universal behavior in these correlators, including a power-law drop-off with distance. We also explore a means of extracting the coefficient of the R^2 term in the low energy effective action, and find that this coefficient may be very large in magnitude, though a calculation in the low energy effective theory is still needed to test this possibility. This result implies that Starobinsky Gravity emerges naturally in the theory, which would have important implications for observational cosmology.

Euclidean Dynamical Triangulations

Running Couplings and Curvature Correlation Functions

by

Scott Bassler

B.S. Applied Physics, Stockton University, 2013

Dissertation

Submitted in partial fulfillment of the requirements for the degree of

Doctor of Philosophy in Physics.

Syracuse University

December 2019

Acknowledgments

I thank my advisor Jack for helping guide me all these years. In working with him I've learned how to code, about lattice techniques, about QCD, about gravity, and all manner of physics I never dreamed would be relevant to the study of gravity. It has been a privilege to work for someone so intelligent and kind.

I thank my professors at Syracuse for the numerous challenging but rewarding classes which I was lucky enough to be in. The long hours on the fourth floor were not in vain!

I thank my fellow graduate students for all of their help on handling assignments and life at Syracuse, both in my year and not, both in my department and not. I cannot hope to list them all, but special thanks go out to Greg, Michael, Craig, Shelby, Kyle, Alex, Raghav, Eric, Lindsay, Ohana, and of course Monica. Graduate school for physics is infamous for being a time that people struggle to find happiness. With all of you, it was easy to find.

I thank Walter for helping me foster my love of teaching at Syracuse, first as his teaching assistant, then as an apprentice at teaching conventions, and soon as a peer.

I thank my undergraduate advisor Neil for convincing me that physics was a path worth following. I cannot help but wonder where I would be without his wisdom, which he gave when I needed it most.

And of course, I thank my family: my mom, my dad, Danny, and Mikey. For all my life, you have supported me in everything I've done, from choir to physics, from Woodbury to Syracuse. I love you all, and couldn't ask for better parents or brothers.

Contents

List of Figures

List of Tables

1 Introduction

1.1 Quantum Field Theory

In the early to mid 20th century, two separate, fundamental theories emerged in physics; quantum mechanics and special relativity. The former established the probabilistic nature of mechanics, wherein particles have indefinite position and momentum. The latter describes how objects at high speeds behave, and how matter and energy are interchangeable.

It became clear from experiments that particles could be created in sufficiently high energy collisions. Nonrelativistic quantum mechanics has no mechanism for new particles to appear, and so a new means of examining the Universe that combined quantum mechanics and special relativity was called for. The result was quantum field theory.

In quantum field theory, or QFT, one particularly useful formulation is the path integral formulation. The fundamental object of consideration is the path integral

$$Z = \int \mathcal{D}\varphi e^{-iS(\varphi)} \tag{1}$$

where φ is a field, which is thought of as existing at every point in space, and quantized excitations of this field are what we refer to as "particles". $S(\varphi)$ is a functional of φ known as the action, which includes the various ways the field(s) interact with one another, and is directly related to the Lagrangian density $S(\varphi) = \int d^4x \mathcal{L}(\varphi)$. The measure $\mathcal{D}\varphi$ calls for there to be contributions from every possible field configuration.

The Boltzmann weight $e^{-iS(\varphi)}$, can be Wick-rotated from Minkowski space to Euclidean space, which amounts to replacing $t \to -i\tau$, so that $e^{-iS_{Minkowski}(\varphi)} \to e^{-S_{Euclidean}(\varphi)}$. Certain problems are easier to solve in Euclidean space, and solutions can be Wick rotated

back to Minkowski space. The Boltzmann weight gives the probability weight for the field configuration φ, and expectation values of observables can be calculated using

$$\langle O \rangle = \frac{1}{Z} \int \mathcal{D}\varphi \; O(\varphi) e^{-S(\varphi)} \tag{2}$$

In practice, the integral itself can seldom be done directly; some approximation is required. For example, the free field theory

$$\mathcal{L}(\varphi) = \frac{1}{2}(\partial\varphi)^2 - \frac{m}{2}\varphi^2 \tag{3}$$

can be solved exactly. However, if an additional term like $\frac{\lambda}{4!}\varphi^4$ is included, the theory becomes interacting and cannot be solved exactly. If the coupling λ is small, then it can be solved perturbatively. This is done by separating the interacting part of the action from the free field theory part

$$S(\varphi) = S_{free}(\varphi) + S_{int}(\varphi) \tag{4}$$

and then expanding $e^{-S_{int}}$ in a power series in λ. This procedure makes it possible to calculate the partition function Z to any order in λ and φ. One can represent terms in this expansion using a set of rules, called the "Feynman Rules", where each term in the expansion can be represented by a Feynman diagram.

In this perturbative expansion, one often encounters integrals such as $\int^{\infty} d^4k \frac{1}{k^4}$ that describe physical observables and yet diverge. This is resolved by asserting that any quantum field theory has a domain of validity beyond which some higher theory takes over. This is captured in the integral by introducing a cutoff μ to the integral, $\int^{\mu} d^4k \frac{1}{k^4}$ so that the infinities become controlled. Introducing a cutoff is a form of "regulating" the infinities of quantum field theory.

However, physical results should not depend on the choice of the cutoff scale, and so any dependence on μ should vanish. Indeed, for *renormalizable* theories, this is the case; one relates the quantities in the theoretical prediction to those in actual experiments so that μ no longer appears. Alternatively, one can view renormalizable theories as those that need only a finite number of counter terms to be introduced to the Lagrangian to cancel any divergences. One can write down theories for which μ cannot be removed from physical quantities. For such theories, there are an infinite number of counter terms that are needed to remove the μ dependence. These theories are called *non-renormalizable*.

An alternative description of the above is that the coupling λ is a function of the cutoff μ, so that each cutoff has its own coupling value such that the observable stays fixed. Coupling constants then are not true constants, but change with energy scale. Quantum electrodynamics (QED), the study of the electromagnetic interaction, features a coupling constant whose value is around $\frac{1}{137}$, though the actual value ois be slightly smaller. However, it turns out that this value isn't the same at all energy scales; it varies with energy scale, increasing as the probed energy scale increases.

For quantum chromodynamics (QCD), which describes the strong interaction, the running of the coupling proves to be of great importance. For low energies, the coupling constant g is large, and a perturbative expansion in g is impossible. However, the coupling constant g runs towards zero for large energies, and becomes non-interacting. This allows QCD to be solved perturbatively at high energies. Because the theory becomes non-interacting in the ultra-violet (UV), QCD is said to be *asymptotically free*.

In the infrared (IR) where QCD is strongly coupled, perturbative methods cannot be used. To study the theory in this regime, non-perturbative methods are required. The most

successful non-perturbative approach to QCD and indeed any quantum field theory, is the lattice, where continuous space is discretized and different field configurations are sampled by randomly exploring the configuration space using numerical Monte Carlo methods. Lattice methods have been used to make many high precision predictions for QCD.

The running of coupling is studied using what is called the *renormalization group*. Generically, a coupling's running is described by a "beta function", which is related to the slope of the running with renormalization scale. For theories like QED where the coupling increases in the UV, this function is positive. However, for theories like QCD that become weakly interacting at high energies, the beta function is negative.

1.2 A Quantum Field Theory of Gravity and Asymptotic Safety

It has long been the goal of physics to describe gravity as a quantum field theory, putting it on the same footing as electromagnetism, the weak force, and the strong force. However, attempts to do so encounter substantial difficulties, most prominently the non-renormalizablility of gravity. In natural units, Newton's Constant G carries mass dimension of -2, and so in the perturbative expansion there appear terms of the form μ/M_{Plank} with ever increasing powers, where μ is the cutoff scale. As this cutoff is taken to infinity, the successive terms would diverge, and physical quantities would become infinite. This can be corrected by the introduction of counterterms, but an infinite number of them would be required, each accompanied by an unknown coupling. An infinite number of experiments would be needed to determine all of the couplings, and the theory would lose predictive power. The appearance of counter-terms has been verified explicitly at 2-loops for pure gravity [1] and 1-loop for gravity with matter fields [2].

A second problem that quantum gravity faces is explaining the smallness of the cosmo-

logical constant. Quantum fluctuations contribute to the vacuum energy of a system, and gravity should see these contributions. Specifically, in effective field theory the gravitational fluctuations should contribute to the cosmological constant at all energies up to the Planck scale. This results in a cosmological constant that is roughly 120 orders of magnitude larger than what has been observed [3].

Weinberg proposed a solution to the first problem called asymptotic safety [4]. If the relevant couplings of a perturbatively non-renormalizable theory approach fixed point values in the UV, the theory would be effectively renormalizable. Should the fixed point value be 0, the theory is asymptotically free, and could be solved perturbatively in the UV by expanding in the small coupling. QCD is the classic example of an asymptotically free theory, and it has enjoyed great experimental success. Asymptotic freedom is just a special case of the more general asymptotic safety.

However, it's possible that the fixed point would occur for some large non-zero value of one or more of the couplings. In this case, a perturbative expansion would become impossible. That gravity cannot be perturbatively renormalized means that it is not asymptotically free, but it might be asymptotically safe. The fixed point values would then be non-zero.

There are three bare parameters in the lattice theory; β, G, and Λ. G is Newton's constant, Λ is the cosmological constant, and β is a free parameter associated with a measure term to be discussed later. In what follows, evidence will be presented that β must be fine tuned. In a lattice theory, symmetries can protect terms from large corrections. If this symmetry is broken by the lattice discretization, that protection is gone, and results cannot be trusted until the symmetry is restored. Usually, this requires the fine-tuning of one or more parameters. We argue that β plays this role in our calculations.

The remaining two parameters, G and Λ, will be shown to not be separately relevant in the renormalization group sense, i.e. their running with energy scale does not contribute to observables. Instead, the combination $G\Lambda$ is relevant. Hence, we argue that the UV critical surface in the vicinity of the fixed point is 1-dimensional, and there is only one relevant, physical coupling. To make predictions, only a single dimensionful parameter is needed to set the scale, and then all other parameters become predictions. The smallness of the cosmological constant might emerge naturally from the theory, even though the mechanism is not apparent.

1.3 Euclidean Dynamical Triangulations

If gravity is asymptotically safe, but is strongly coupled in the UV, then one must evaluate the theory non-perturbatively. Lattice methods are the best for calculations, since they are the best known means for giving controlled answers. For any asymptotically safe theory on the lattice, the fixed point would manifest as a continuous phase transition with a finite-dimensional UV critical surface. A continuous phase transition ensures a divergent correlation length, allowing one to take a continuum limit. This limit would be defined by the approach toward the critical point.

To implement gravity on the lattice, one must evaluate the path integral by summing over all possible geometries. To do this, continuous, curved space-time must be discretized into discrete, piece-wise linear simplices. The earliest attempt at this was called Regge Calculus. This approach breaks up continuous space in d-dimensions into d-dimensional simplices, the analogue of triangles in d-dimensions (The 2-simplex is a triangle, the 3-simplex a tetrahedron, etc.) with varying edge lengths. In Regge Calculus, the triangulation is fixed and the dynamics is encoded in the varying edge lengths [5].

Euclidean Dynamical Triangulations (EDT) was developed from Regge calculus [7][6].

Rather than allowing the edge lengths to vary, all simplices have fixed, equal edge lengths, so that all of the dynamics is in the connectivity of the simplices. The advantage of this approach is that it is argued to correctly count each physical geometry, which should in turn maintain continuum diffeomorphism invariance. This has been confirmed in 2 dimensions, where EDT reproduces continuum results with high precision [8].

EDT has been studied for several decades, and even explored in 4d. However, there it met less success than in 2d. It was found that although a phase transition did exist, the transition was first-order rather than second-order [13] [14]. Of these two phases, one consisted of geometries with a few highly connected vertices and seemingly infinite fractal dimension and has been dubbed the collapsed phase, while the other's geometries have branched polymer-like minimal necks and fractal dimensions below 4. Neither of these phases resemble semi-classical gravity. [9]-[12]

An attempt was made to salvage the theory by including a non-uniform weighting term to the path integral measure with an accompanying free parameter β [15] [16]. This led to an expanded phase diagram with a phase transition line, and a seemingly new phase, dubbed the crinkled region. However, the phase transition line proved to be first order, and the new phase appeared to be an extension of the collapsed phase rather than a genuinely separate phase, and was likely nothing more than the familiar phase with large finite-size effects [17] [18].

A variant of EDT, called Causal Dynamical Triangulations (CDT), was developed. In CDT, time-like links are distinguished from space-like links, allowing a foliation into space-like hypersurfaces to be introduced. The spatial topology is then fixed, so branching into baby universes is prohibited. This preserves unitarity, and an explicit time coordinate allows a well-defined Wick rotation. This approach has had many positive results, most notably

the appearance of a de Sitter like space of dimension four [19] [20]. However, this approach explicitly breaks space-time symmetry, and therefore it is unclear if the continuum limit of CDT is indeed general relativity. It may be that CDT amounts to a partial gauge-fixing, in which case some variant of EDT should also be viable. This warrants another exploration of EDT, where space-time symmetry is maintained. If the two approaches can be shown to be in the same universality class, then the attractive features of CDT (Unitarity) and EDT (space-time symmetry) would be common to both.

In this new look at EDT, the non-trivial measure term is reinterpreted. It is argued that the lattice regularizataion breaks general coordinate invariance. As symmetry breaking by the lattice must be restored by the fine tuning of a parameter, it's argued that the measure term must be fine-tuned to restore this broken symmetry. Once this is done, evidence is found that the correct physics emerges upon taking the lattice spacing to zero, and the lattice volume to infinity.

In this work, we begin by reviewing the implementation of EDT in four dimensions, and the principle features of the model in section 2. In section 3, we examine the running of the couplings of the theory to provide evidence that asymptotic safety is realized, and identify which parameters are relevant to the theory. In section 4, we study the curvature two-point correlation functions using two different discretizations of curvature. Both approachs are compatible with a power law fall-off, thus giving the same universal behavior for this function. We argue that the continuum extrapolated function could be used to constrain the couplings of the continuum low energy effective theory of gravity. If the study done here holds up to further scrutiny, it may have important implications for inflation. We conclude in section 5.

2 The Lattice Formulation

2.1 The Discretized Action

The action for General Relativity in four dimensions is the Einstein-Hilbert action

$$S_{EH} = -\frac{1}{16\pi G}\int d^4x\sqrt{g}(R - 2\Lambda) \tag{5}$$

with G Newton's Constant, Λ the Cosmological Constant, R the Ricci Scalar Curvature, and metric g. We have Wick rotated to a Euclidean metric. The Euclidean path integral is

$$\mathcal{Z}_E = \int \mathcal{D}g\sqrt{g}^{\beta}e^{-S_{EH}} \tag{6}$$

where the sum is over metrics, or equivalently over universe geometries. The $\sqrt{g}^{\beta}$ is the measure term with free parameter β.

The lattice implementation discretizes space-time into regular, piece-wise linear simplices. In four dimensions, these pieces are pentachorons or 4-simplices, the 4d equilateral triangle. The discretized action, the Einstein-Regge action, is [5]

$$S_{ER} = -\kappa\sum_{j\in N_2} V_j\delta_j + \lambda\sum_{i\in N_4} V_4 \tag{7}$$

where the first sum is over the triangles and the second is over 4-simplices. $\kappa = \frac{1}{8\pi G}$ and $\lambda = \kappa\Lambda$. Performing the sums with the aid of some topological identities gives

$$S_{ER} = -\frac{\sqrt{3}}{2}\pi\kappa N_2 + \left(\kappa\frac{5\sqrt{3}}{2}\arccos(1/4) + \frac{\sqrt{5}}{96}\lambda\right)N_4, \tag{8}$$

where N_2 and N_4 are the number of triangles and 4-simplices, respectively. We define $\kappa_2 = \frac{\sqrt{3}}{2}\pi\kappa$ and $\kappa_4 = \kappa\frac{5\sqrt{3}}{2}\arccos(1/4) + \frac{\sqrt{5}}{96}\lambda$, so that the action can be written succinctly

as

$$S_{ER} = -\kappa_2 N_2 + \kappa_4 N_4 \tag{9}$$

The parameters κ_2 and κ_4 are the inputs to the lattice simulations. These definitions can be inverted to get G and Λ in terms of κ_2 and κ_4.

As for the measure term, it becomes

$$\sqrt{g}^{\beta} \to \prod_{j}^{N_2} \mathcal{O}_j^{\beta} \tag{10}$$

where $\mathcal{O}_j$ is the order of triangle j, or the number of simplices triangle j is a sub-simplex of. In practice, this term is exponentiated and included within the action.

2.2 Constructing Geometries

Each geometry is made by gluing together 4-simplices in different arrangements along their tetrahedral faces. To compute the path integral, the space of all geometries is explored by a random walk. To achieve this, new geometries are generated by modifying existing geometries. The new geometry must remain valid triangulations, must maintain the same topology as the original configuration, and it must be possible for any valid geometries to be accessible to the random walk, i.e. the process of generating new geometries must be ergodic.

The alterations that satisfy these requirements are the Pachner Moves, a set of ergodic triangulation altering moves [6] [21]. In a d-dimensional triangulation, the d+1 moves work by selecting an i-dimensional simplex, where i can be any integer from 0 to d, and replacing it with a $(d-i)$-dimensional simplex, provided this results in a valid triangulation. In 2 dimensions, the three moves are deleting a node, flipping a link (A move which is its own

inverse), and inserting a node. In 4 dimensions, the five moves are deleting a node, replacing a link with a tetrahedron, flipping a triangle, replacing a tetrahedron with a link, and inserting a node. In two dimensions, node insertion and link flipping are both guaranteed to be possible for any given i-simplex, but in four dimensions, only the node insertion move is guaranteed to be possible.

The starting point for the random walk is the minimal 4-sphere, the triangulation with the topology of a sphere in 4-dimensions and the smallest number of simplices. This consists of six 4-simplices interconnected. From this starting configuration, the Pachner Moves are applied to build up the full geometry. Note that the Pachner moves preserve topology, but not volume.

The geometry updates are accepted or rejected via a metropolis algorithm. A random move is selected, and the change to the action of the proposed move is calculated. Then a random number between 0 and 1 is generated. If the random number is less than the Boltzmaan weight corresponding to the change in the action, the move is accepted and the geometry is updated. If not, the move is rejected. In this way, detailed balance is preserved.

In order to take the infinite volume limit, one must generate lattices of different volumes but with the same lattice spacing. Large volumes are exponentially suppressed, and so it is computationally difficult to obtain geometries with the needed volume while simulating with fixed cosmological constant and variable volume. Instead, we simulate at fixed volume. To achieve a fixed volume, κ_4, which corresponds to the bare cosmological constant, is adjusted dynamically as the geometries are updated. However, in order for the Pachner moves to be truly ergodic, the volume must be allowed to fluctuate away from its designated value. One extra term is added to the action, $\delta\lambda|N_{4_f} - N_4|$, which allows the volume to wander about its designated value. This restriction introduces a systematic error proportional to $\delta\lambda$, so for

small $\delta\lambda$, the error is negligible. $\delta\lambda = 0.04$ is used throughout this work.

2.3 Degenerate Triangulations

The original implementations of EDT employed combinatorial triangulations, in which all structures are uniquely defined by their vertices. This means that no two simplices share all of their vertices, nor do any two tetrahedra, triangles, or links. Using combinatorial triangulations it was originally thought that the transition was second order because tunneling effects did not emerge until volumes of 32k 4-simplices or larger.

It was later realized the the combinatorial constraints could be relaxed to a wider set of triangulations, called degenerate triangulations [22]. Nodes remain unique, but links, triangles, tetrahedra, and simplices are no longer uniquely defined by their nodes. It was found that degenerate triangulations reduced finite size effects by approximately an order of magnitude, observed first in two dimensions and later in four dimensions. As a result, it became possible to identify the phase transition for lattices with around 4k simplices [18]. Following this success, and since the choice of discretization is unlikely to affect continuum physics, geometries in this work are degenerate.

2.4 Phase Diagram

To study the resultant geometries, it is useful to define their fractal dimensions. One definition is the Hausdorff dimension, D_H, determined from how a sphere scales in the given space as its radius goes to zero

$$D_H = \lim_{r \to 0} \frac{\log(V)}{\log(r)} \tag{11}$$

Another fractal dimension is the spectral dimension, related to the return probability, $P_r(\sigma)$ for a random walk beginning at a given point in the geometry to return to its starting point:

$$D_s(\sigma) = -2\frac{d\log\langle P_r(\sigma)\rangle}{d\log\sigma} \tag{12}$$

In general, the Hausdorff and spectral dimensions are not the same for a fractal geometry. Agreement only emerges for sufficiently smooth geometries.

The inclusion of the non-trivial measure term, $\sqrt{g}^{\beta}$, expands the phase diagram to become two dimensional. Two distinct phases have been observed, separated by a first order phase transition line. The crinkled region is separated from the collapsed phase by a crossover. A schematic phase diagram is shown in figure 1.

For small κ_2 and small β, the geometries are in the collapsed phase. This phase is characterized by a small number of nodes shared by many simplices, and a low number of steps needed to traverse the entire lattice. The Hausdorff and spectral dimensions in this phase are both large, perhaps even infinite in the infinite volume limit. The curvature of this phase is large in magnitude, but is negative [23]. This phase is inconsistent with what one needs for a theory of gravity.

Within the collapsed phase is the"crinkled region", which shares features from both phases, but is separated from the collapsed phase by a crossover rather than a transition, so that it is not distinct from the collapsed phase. It is likely just the collapsed phase with large finite-size effects. Study of the fractal dimensions in this region showed that the Hausdorff dimension was much greater than four, which is consistent with the collapsed phase, and the spectral dimension for large distances was also greater than four and increased with volume [17] [18]. These features of crinkeled region make it inconsistent with semi-classical gravity

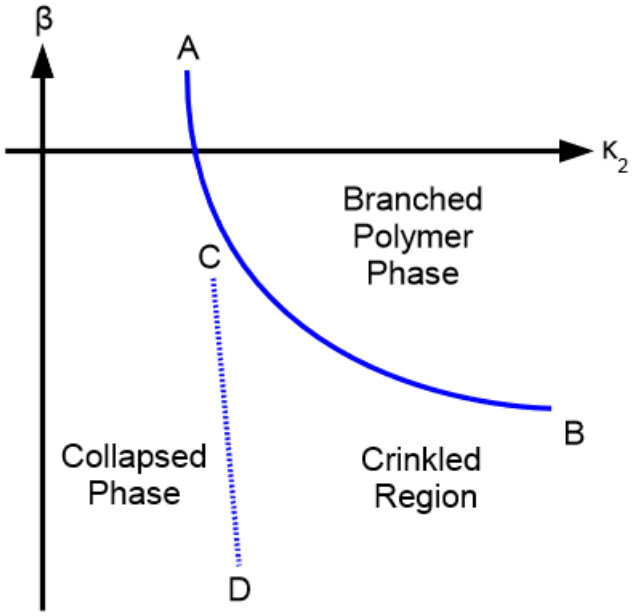

Figure 1: A schematic view of the phase diagram for EDT as a function in the $\kappa_2 - \beta$ plane.

as well.

For large κ_2 and $\beta \gtrsim -1$, the geometries are in the branched polymer phase. This phase is characterized by so-called "baby universe" tails, elongated extensions off the "mother universe" with minimal necks. The Hausdorff dimension in this phase is 2, whereas the spectral dimension is $\frac{4}{3}$ [17] [18]. This phase is also inconsistent with our world.

A similar phase diagram is found when using the Wilson Fermion discretization in QCD. For Wilson Fermions, the lattice regulator breaks chiral symmetry, which is approximately restored upon tuning the bare fermion mass to its critical value. The critical value is different for each lattice spacing, and higher values of β (the inverse of the strong coupling, α_s) correspond to finer lattices. Hence, to get the correct, continuum behavior, one must take β to infinity while tuning the inverse bare mass to keep β at its critical value. In other words, one must follow the first-order line to infinity to find a higher-order critical point. A

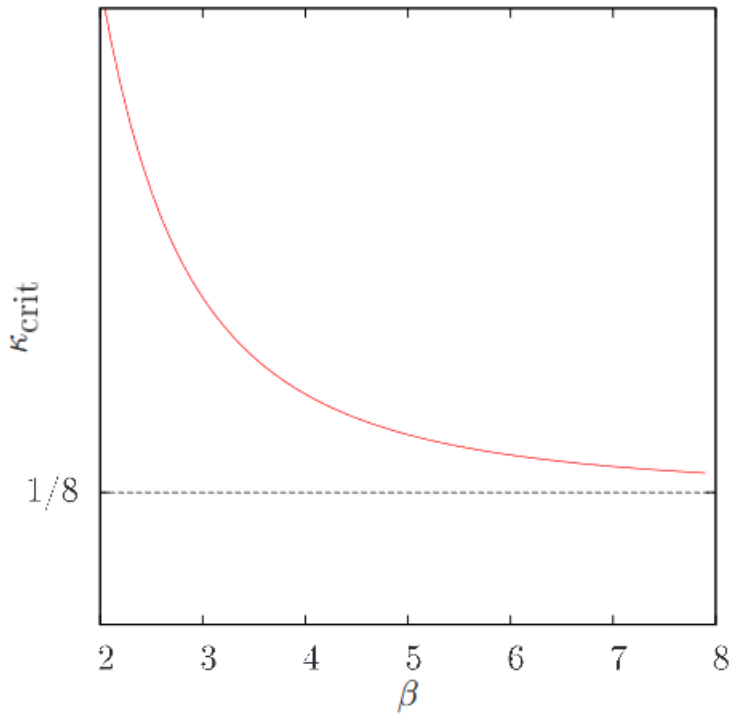

Figure 2: The phase diagram for QCD with Wilson fermions in the $\beta - \kappa$ plane. β is the inverse strong coupling constant, $1/\alpha_s$, and κ is the inverse bare fermion mass.

schematic diagram of the phase diagram for QCD with Wilson Fermions is given in figure 2. Given the similarity between the two phase diagrams, we follow the same approach for EDT as one would in lattice QCD to attempt to extract useful physics. Early studies of EDT found that the Hausdorff dimension was close to four near the transition, providing some further motivation to investigate this part of the phase diagram.

This is the procedure we implement for EDT. For each lattice volume and value of β, several values of κ_2 are tested. If the geometries are near the transition, there will be a tunneling between the two phases, which can be observed in the Monte Carlo history of N_0. The κ_2 value which results in a histogram with two peaks of roughly even height is the tuned value for the given β value. However, this procedure requires several tunneling events to reduce the systematic effects associated with determining this value, and the tunneling

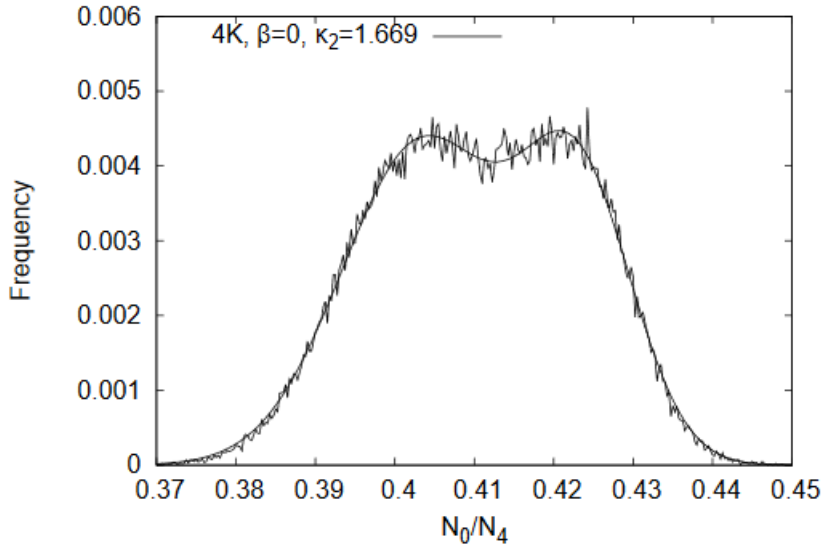

Figure 3: This histogram of N_0 for the 4k $\beta = 0$ ensemble, with a clear double guassian structure. That the two peaks are the same height indicates that the ensemble is correctly tuned to the phase transition

probability is exponentially suppressed with volume. Hence, for large volumes, a different procedure that uses a global, rather than local, observable is used. In the next subsection, a definition is given for the volume-volume correlator c_{N_4}, the peak of which acts as our global observable. The phase transition occurs at the value of κ_2 that has the largest slope in the plot of the peak of c_{N_4} vs κ_2. A plot showing the N_0 histogram for the 4k $\beta = 0$ ensemble that demonstrates the transition is found in figure 3 and the correlator peak method for both the 16k and 32k ensembles at $\beta = 0$ are shown in figure 4.

In lattice QCD with Wilson Fermions, only one of the phases is physical. Likewise, in lattice quantum gravity it's found that semiclassical behavior only manifests if the phase transition line is approached from the left, in the collapsed phase. It turns out that near the transition, the collapsed phase is qualitatively different from that deep within the collapsed phase, with fractal dimensions that may be consistent with 4 [9] [12]. Evidence for this is presented in sections 2.5.1 and 2.6.2. When tuned to the transition line, the tunneling

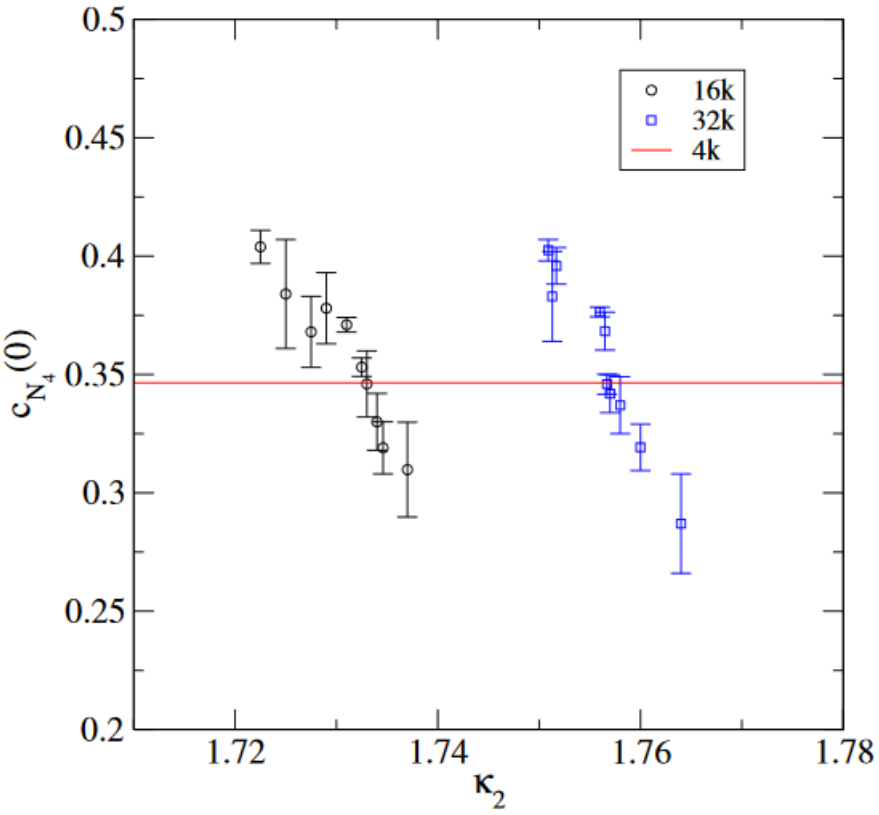

Figure 4: A plot of the peak of the volume correlator, $c_{N_4}(0)$, for both the 32k and 16k $\beta = 0$ ensembles. The value of κ_2 that maximizes the slope is the critical value of κ_2. The red line shows the critical value for the 4k $\beta = 0$ ensemble, which should agree with the 16k and 32k ensembles if the correct Hausdorff dimension is chosen. That there is good agreement suggests that the chosen value of 4 is correct.

discussed above means that some of the geometries will be in the correct, collapsed phase, while others will be in the unphysical branched polymer phase. Whether the run is in the correct phase can be determined by looking at the history of N_0/N_4, which will be smaller in the more highly connected collapsed phase. A plot showing three such histories for ensembles with $\beta = 0$ and three different volumes is given in figure 5. Only those configurations in the correct phase are used for calculations.

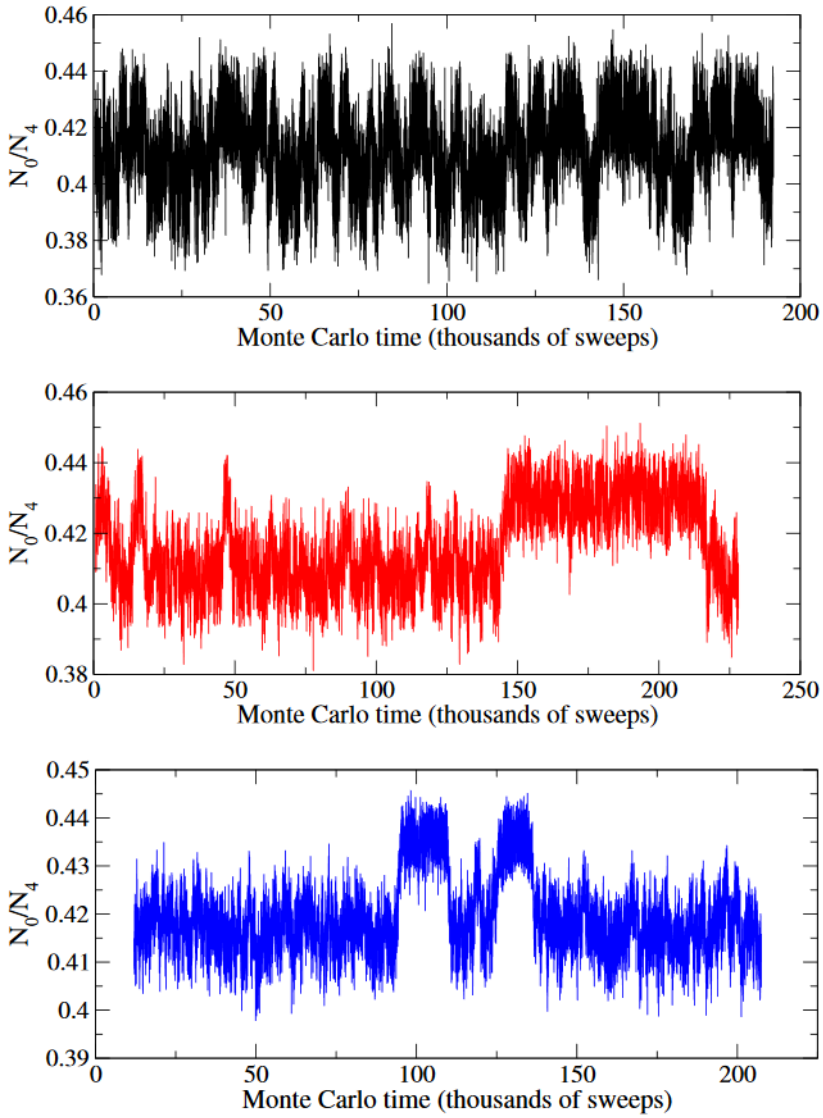

Figure 5: The history of the quantity N_0/N_4 in Monte Carlo time at $\beta = 0$ for three different volumes. From top to bottom, the volumes are 4k, 8k, and 16k.

2.5 Evidence for Classical Behavior

2.5.1 Global Hausdorff Dimension

The global Hausdorff Dimension can be studied using finite-size scaling of correlation functions. There are two correlators we consider in this section. The first is

$$C_{N_4}(\delta) = \sum_{\tau=1}^{t} \frac{\langle N_4^{shell}(\tau) N_4^{shell}(\tau+\delta)\rangle}{N_4^2} \tag{13}$$

defined in [18] to be similar to one defined in CDT [20]. $N_4^{shell}(\tau)$ is the number of four simplices in a spherical shell one 4-simplex thick a geodesic distance τ from a randomly selected simplex. The geodesic distance is obtained by determining how many "hops" it takes to traverse from one simplex to another by going to its nearest neighbors. The parameter t is the maximum number of shells. The correlator is normalized according to

$$\sum_{\delta=-t}^{t} C_{N_4}(\delta) = 1 \tag{14}$$

This correlator gives a measure of the shape of the lattice geometry. The correlator can be rescaled by defining $x = \delta/N_4^{1/D_H}$ to obtain the universal distribution

$$c_{N_4}(x) = N_4^{1/D_H} C_{N_4}(N_4^{1/D_H} x) \tag{15}$$

If the correct value of D_H is chosen, then this universal distribution is independent of volume. This rescaled distribuion is plotted for three volumes at $\beta = 0$ in figure 6 with $D_H = 4$. That the curves lie on top of one another suggests that the correct value of D_H is close to 4. A fit designed to maximize the overlap treating D_H as a free parameter found that $D_H = 4.1 \pm 0.3$ where the error is only the statistical.

We also consider the function $N_4^{shell}(\tau)$ directly. This quantity can be interpreted as the three-volume as a function of Euclidean time τ. Performing a similar rescaling and defining $\rho = \tau/N_4^{1/D_H}$, we have

$$n_4(\rho) = 1/N_4^{1-1/D_H} N_4^{shell}(N_4^{1/D_H}\rho) \tag{16}$$

Like the volume correlator above, this function should be invariant if the correct D_H is chosen. Once again, the value $D_H = 4$ appears to be correct. A plot of this function for the same three volumes at $\beta = 0$ appears in figure 7. Again, the overlap confirms that the global

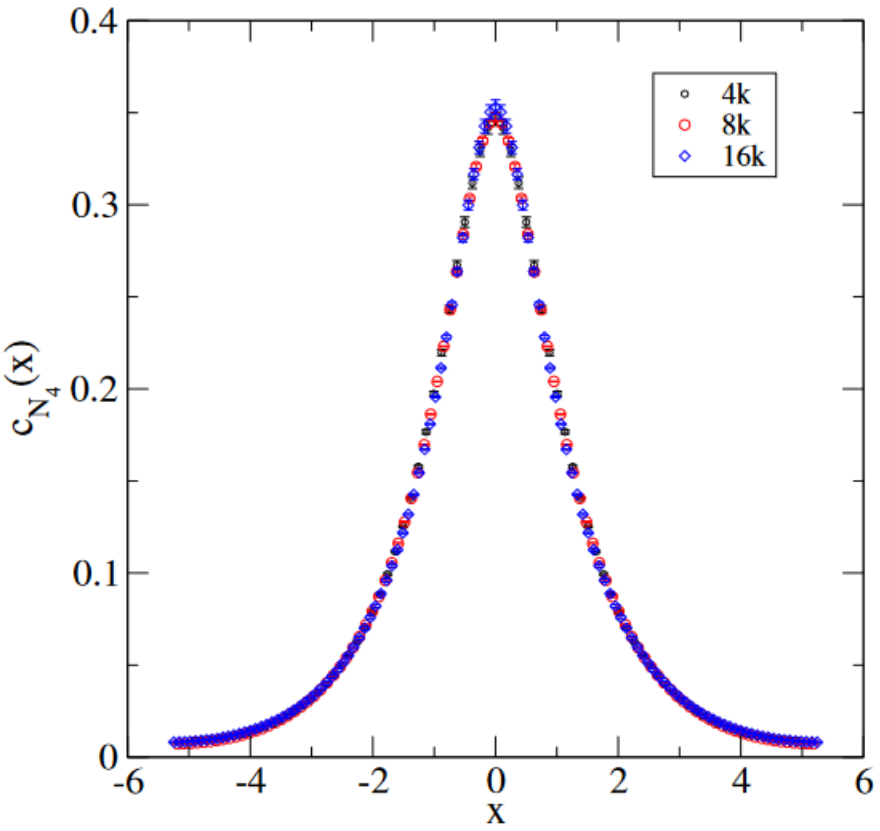

Figure 6: The volume distributions, $c_{N_4}(x)$, for three different volumes at $\beta = 0$, after rescaling assuming a Hausdorff dimension of 4.

Hausdorff dimension is close to 4.

2.5.2 The de Sitter Solution

The second function, $n_4(\rho)$, gives the three-volume as a function of Euclidean time, and thus has a straight-forward classical prediction. Euclidean de Sitter space in four dimensions is a 4-sphere, which is the same topology as the generated geometries, though there is no guarantee that the geometries will be a symmetric 4-sphere; the un-physical phases are quite distinct from the 4-sphere despite having the same topology. The classical prediction for

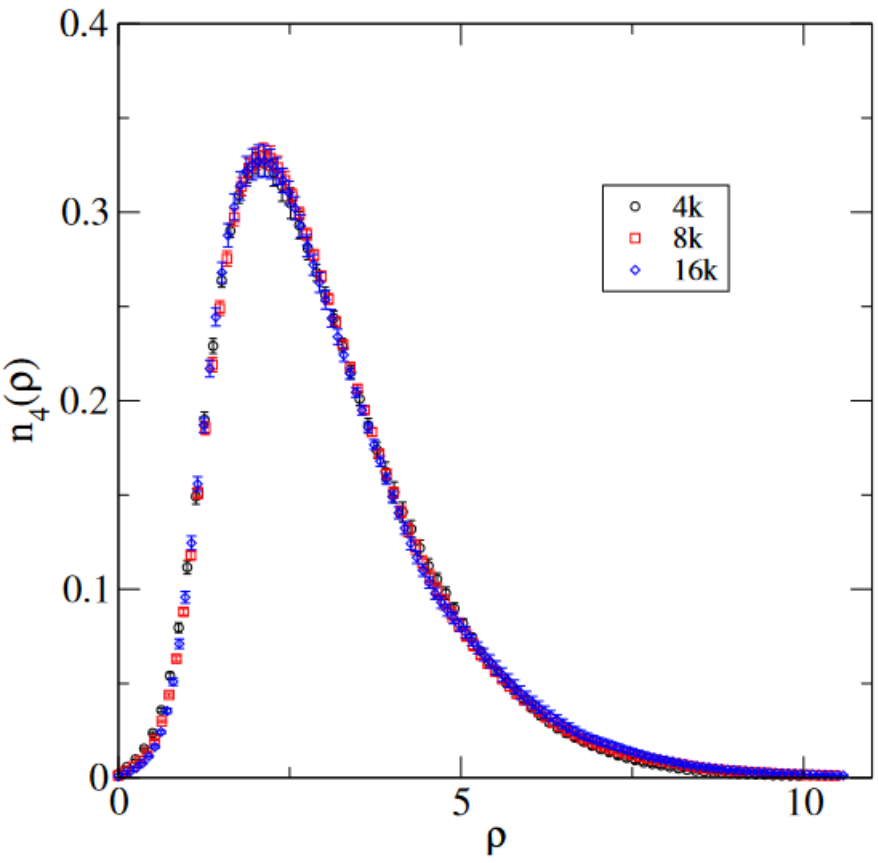

Figure 7: The volume distributions, $n_4(\rho)$, for three different volumes at $\beta = 0$, after rescaling assuming a Hausdorff dimension of 4.

Euclidean de Sitter space is

$$N_4^{shell}(i) = \frac{3}{4} N_4 \frac{1}{s_0 N_4^{1/4}} \sin^3\left(\frac{i}{s_0 N_4^{1/4}}\right) \tag{17}$$

where i is the Euclidean time in lattice units, and s_0 is a free parameter.

A plot of the function $n_4(\rho)$ for several values of β, as well as this classical prediction, is shown in figure 8. The lattice data has been rescaled to show the qualitatively good agreement with the classical solution before the classical turning point. Beyond this point, the lattices have a long tail that the classical solution does not.

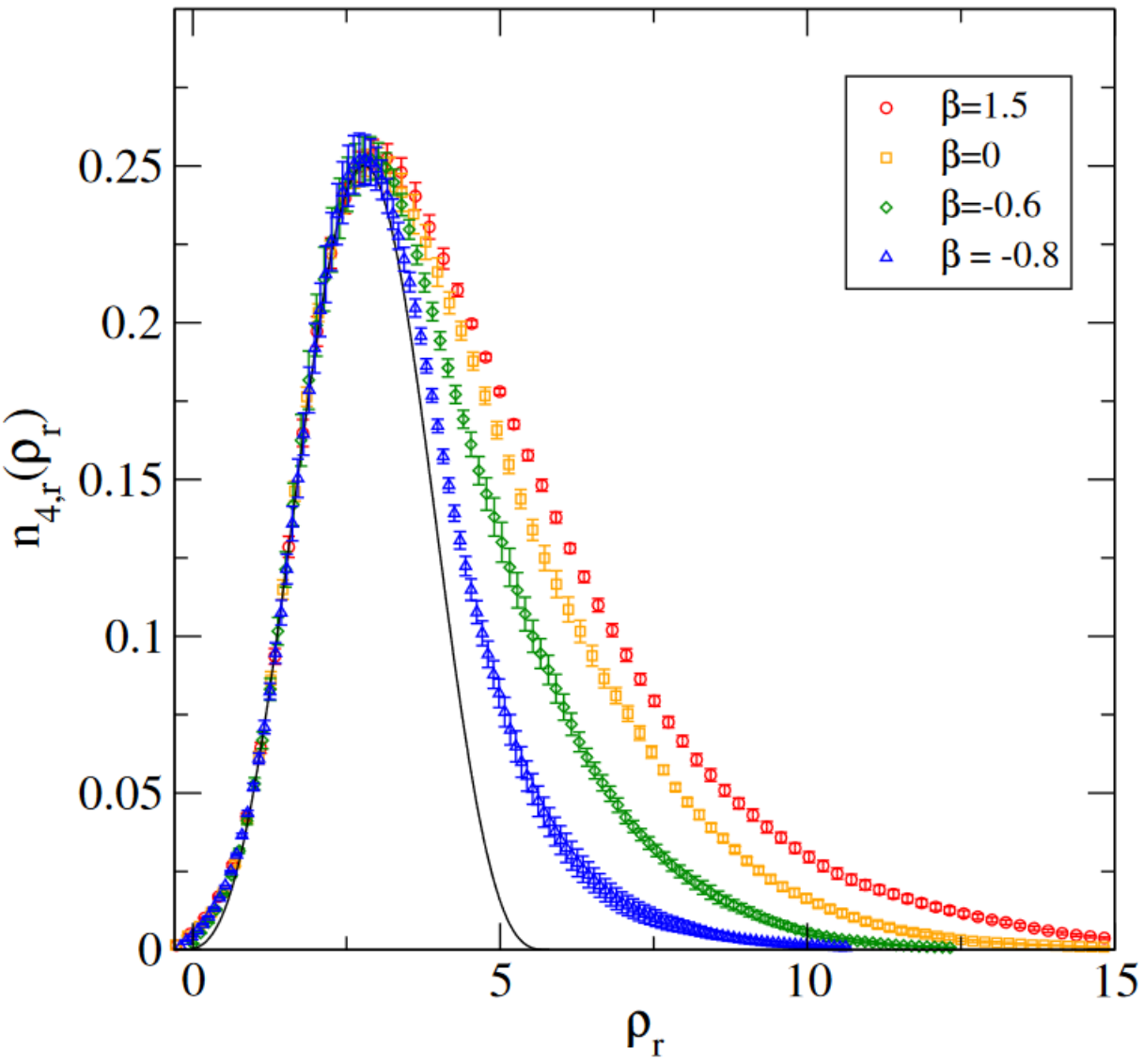

Figure 8: The rescale $n_4(\rho)$ distribution for several different β values, and therefore several different lattice spacings, as well as the de Sitter solution in black. As the continuum limit is taken, the lattice data gets closer to the de Sitter solution.

In the next section, a procedure for determining the relative lattice spacing between configurations will be established. In anticipation of this procedure, the ensembles are ordered in the plot in figure 8 by their relative lattice spacing. As the lattice spacing is taken to smaller values, the un-physical tails decrease and become closer to the classical prediction. It

is presumed that this is caused by the baby universe tails, which diminish with finer lattice spacings. This can be visualized using a network visualization tool, as in figure 9 [26]. For coarse lattices, there is a very clear dense ball with distinct branches shooting off from it which can be interpreted as baby universes. As the lattice spacing is reduced, the amount of the lattice in the bulk core increases, until for the finest lattices it becomes difficult to even distinguish the core from the branched structure.

Thus, it is likely that the asymptotic tail in the volume distribution is a cutoff effect. One might find it odd that a cut-off effect leads to a distortion of long distance physics, but this is known to happen when the lattice regulator breaks a symmetry that matters at long distances. As an example, when chiral symmetry is broken for Wilson fermions, this leads to cutoff effects impacting long distance behavior. In the continuum limit, these cut-off effects vanish [24]. This suggests that the lattice regulator for EDT also breaks some important symmetry. We conjecture that this is the diffeomorphism invariance of general relativity.

In CDT, 4-dimensional Euclidean de Sitter space has also emerged as a solution. In that approach, good agreement with the classical prediction is found in what has been dubbed the "extended" phase of CDT [25]. If EDT and CDT are in the same universality class, they must agree on continuum results, even if they disagree at finite lattice spacing. That the volume distribution approaches the classical prediction in the continuum for EDT, which also agrees with the results from CDT, is evidence that the two approaches may indeed be in the same universality class.

2.6 Towards the Continuum Limit

As discussed above, semi-classical behavior emerges for lattice quantum gravity if the geometries are tuned to be to the left of but sufficiently close to the phase transition line. As β is decreased, the κ_2 value needed to be on the critical line grows to larger values. As κ_2 is

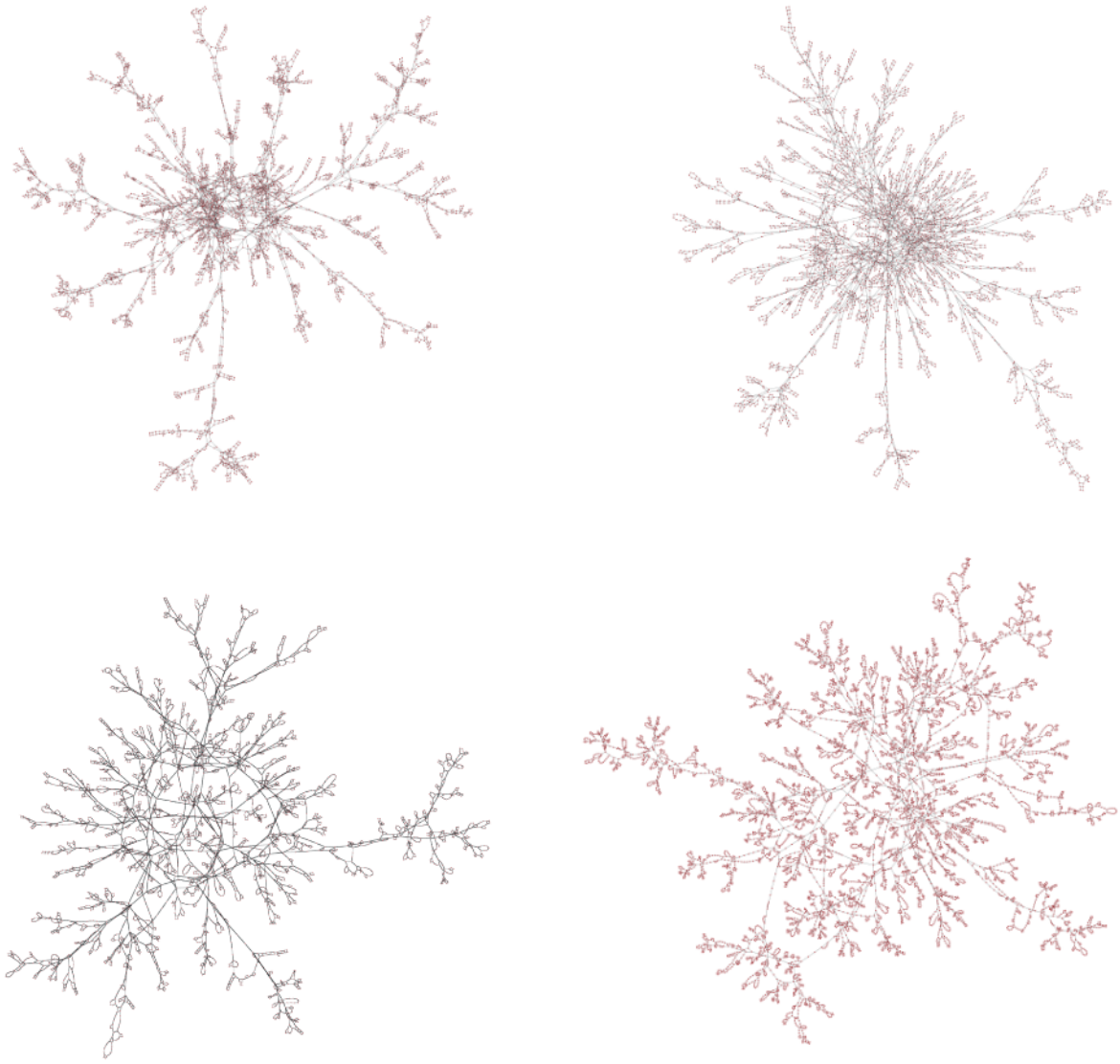

Figure 9: A visualization of the geometries using a network visualization tool. The top left geometry is the coarsest at $\beta = 1.5$, the top right is the second coarsest at $\beta = 0$. The bottem left is the second finest at $\beta = -0.6$, and the bottom right is the finest at $\beta = -0.8$. For the coarser lattice, the baby universe branchings are easily identified as separate from the bulk, but this distinction diminishes for finer lattices.

taken to be larger while still close to the critical line, the latent heat of the phase transition, as measured by the separation between the peaks in the N_0/N_4 histogram, decreases. That the phase transition softens with large κ_2 provides hope that the first order phase transition line does indeed end at a continuous phase transition point. However, exploring this region of the phase diagram proves difficult, as large κ_2 values lead to long autocorrelation times

and large finite-size effects.

Whether or not the fixed point, if it exists, occurs at finite or infinite κ_2 makes no difference as to whether or not gravity is asymptotically safe, but has important implications for the interpretation provided here. If the critical point exists for a finite (κ_2, β) pair, then many different trajectories can reach this fixed point, and no fine-tuning of the lattice parameters would be necessary [27]. On the other hand, if the critical point is at infinite κ_2 with finite β, then only one possible trajectory can lead to the critical point, i.e. a fine-tuning of the parameters. Neither scenario can be ruled out at present, but the arguments herein pertaining to the need for a fine-tuning suggest that the critical point is at infinite κ_2.

Some previous EDT studies provide evidence on this account. In three dimensions with a non-trivial measure term of the kind considered here, a phase diagram similar to the one in four dimensions is found [28]. If that model's analogue of κ_2 is taken to be large, the strong coupling expansion can be used. However, the expansion breaks down due to large finite-size effects around the phase transition at $\beta = -1$ [29], which is around the value of β that appears to be consistent with what the tuning in four dimensions requires.

Further evidence comes from a study that considers a color-tensor model [30]. This model is argued to be equivalent to EDT in the infinite κ_2 limit. The model finds that there are two phases separated by a continuous, third-order transition. If the equivalence of this model and infinite κ_2 EDT is maintained, this strengthens the idea that the critical line ends in a higher-order critical point. If correct, this would ensure that a continuum limit can be taken in our model.

In this section, further evidence of a continuum limit being possible for EDT is provided. A method of determining the relative lattice spacing is put forward, and is shown to be

consistent with the procedure of reducing the latent heat and lattice artifacts. The spectral dimension is shown to be consistent with 4 in the infinite volume, continuum limit, and for short scales $D_s \approx 3/2$, which may provide a resolution for an apparent contradiction between renormalizable gravity and black hole entropy scaling.

2.6.1 Setting the relative lattice spacing

To obtain the lattice spacing, one would use a dimensionful quantity with small discretization errors that is not influenced by finite-size effects. This amounts to determining the renormalized Plank mass. The natural choice of a dimensionful parameter is G. This presents difficulties, since it requires making contact with the semiclassical physics while maintaining the requirement that the lattice spacing is much smaller than the Plank length, which is itself smaller than the extent of the lattice. That the geometries that emerge are de Sitter like is insufficient to determine the lattice spacing, since G does not appear in the classical de Sitter solution. An alternative strategy would be to examine the semiclassical fluctuations about de Sitter space, since that does include G [25] [31], but the lattice geometries studied here are too small and too coarse for this to be done with precision. Even so, calculations using this approach suggest that the finest lattice spacing is a factor of 3 to 5 smaller than the Plank length.

In light of this, the absolute lattice spacing will be left for future work. We still need to determine the relative lattice spacing, which can be found using an unphysical quantity that is not necessarily related to the classical limit. One such parameter is the return probability, calculated to determine the spectral dimension in Eq.(12). If the diffusion time is a universal physical quantity, it can be used to set the relative lattice spacing. Since the physical volumes are small, it is convenient that the return probability is fairly insensitive to volume. A plot of the return probability vs diffusion time for several lattice volumes at

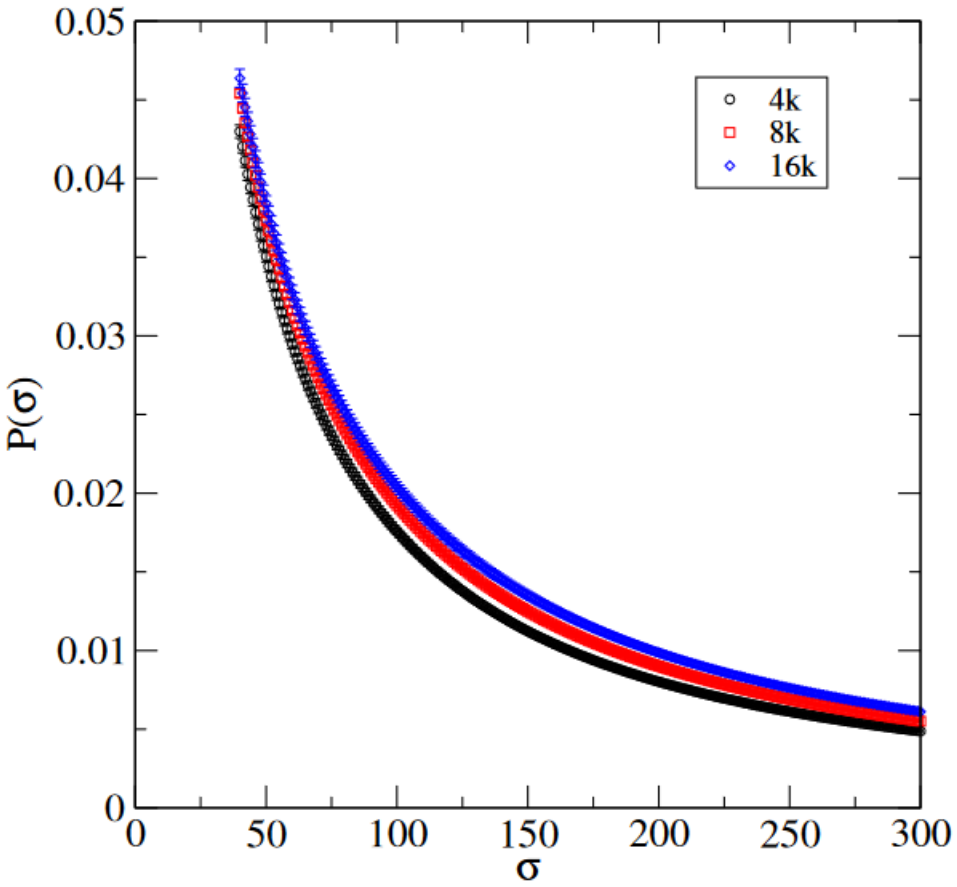

Figure 10: The return probability as a function of diffusion time σ for three different volumes at $\beta = 0$. This appears to be insensitive to volume.

$\beta = 0$ confirms that the variation with volume is small. This is shown in figure 10.

For configurations at different values of β, all of which are tuned to be close to the transition line, there is much greater variation between the curves, as shown in figure 11. The diffusion time has dimension of length squared, and so should scale with lattice spacing squared as the continuum limit is taken, based on the d-dimensional diffusion equation [32]. The diffusion time σ for each curve can be rescaled to $\sigma_r = \sigma a_{rel}^2$, so that the curves lie on a universal curve. This is demonstrated in figure 12. The best agreement is demanded to be at $\sigma_r \approx 100$, since smaller values suffer from discretization errors, and larger from finite-size effects.

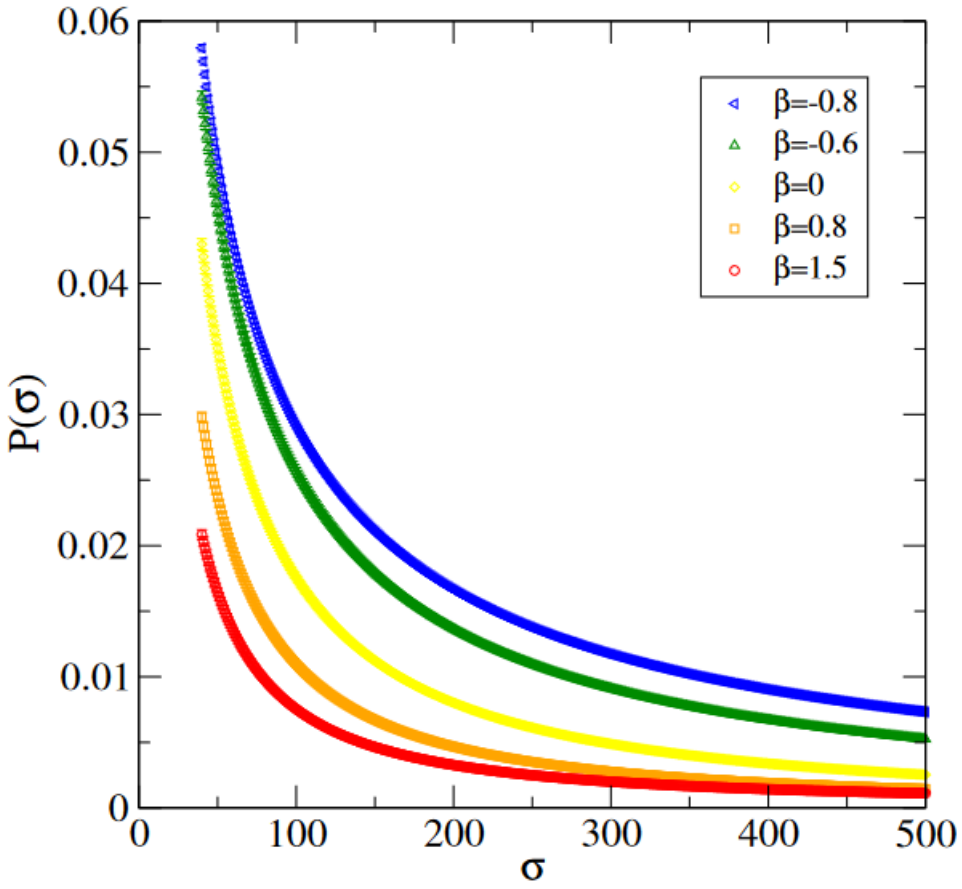

Figure 11: The return probability as a function of diffusion time σ for many different β values.

The factor by which σ must be rescaled to obtain the universal curve is used to determine the relative lattice spacing. For this procedure to work, the variation of parameters in the bare action must follow a line of constant physics, which is the case for this model if the arguments that the broken symmetry necessitates a fine-tuning and the number of relevant couplings found in the next section is correct. The difference in rescalings for different volumes is used to estimate a systematic error. The results for the relative lattice spacings are given in Table 1. We see that taking κ_2 to larger values corresponds to decreasing the lattice spacing.

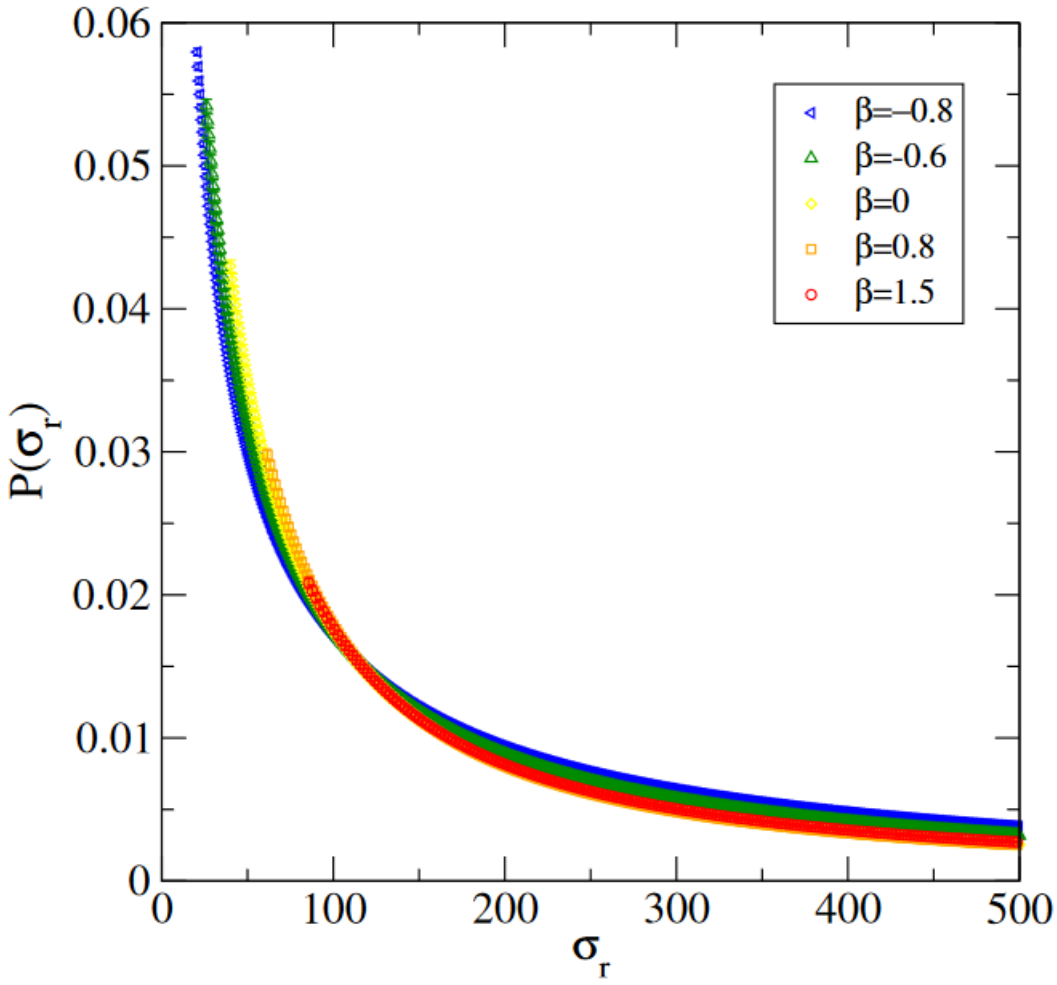

Figure 12: The return probability P_s as a function of rescaled diffusion time σ_r for many different β values, where the rescaling is such that the different curves lie on top of one another. The amount by which σ must be rescaled gives the relative lattice spacing.

2.6.2 The Spectral Dimension

Another quantity of interest to study is the spectral dimension. Other studies of the spectral dimension have shown that it varies as a function of the distance scale that you are probing, and that it tends to a value of close to 2 for small distances, and around 4 for large distances [20] [33] [34] [35]. This is crucial, as the Hausdorff and spectral dimensions do not agree in general, but must both be 4 at long distances to recover the correct classical limit. CDT has also obtained this result, providing additional evidence that the two approaches are in the same universality class. There is also an argument against the asymptotic safety of gravity

Volume	β	κ_2	Number of configurations	a_{rel}
16k	0	1.7325	1387	1
8k	0	1.7024	2500	1
4k	0	1.669	920	1
4k	1.5	0.5886	523	1.47(10)
8k	-0.8	3.0	1975	0.72(5)

Table 1: Test The relative lattice spacing of each ensemble in relation to the $\beta = 0$ ensembles.

that can be resolved if the spectral dimension takes on the value of 3/2 for small distance scales. This was found to be the case in CDT [36], and the current analysis suggests this is the case for EDT as well.

The spectral dimension is defined in Eq.(12) from the return probability of a random walk on the dual lattice, i.e. the likelihood of returning to the randomly selected starting point of your walk after a given number of steps σ. The baby universe tails present an issue here, since they are an unphysical discretization error, and so their contributions to measurements should be minimized. To accomplish this, the starting simplex for the random walk is selected to be in the bulk universe rather than in the baby universe tails. These simplices are those that are found in the largest shell around a randomly selected simplex. An analgous method is used in CDT, where the random walk is started in the time slice with the greatest three volume, to avoid sampling the cutoff size stalk in the time direction.

Figure 13 shows a plot of the spectral dimension as a function of σ for the 8k $\beta = 0$ ensemble, as well as a fit to the distance dependence of the spectral dimension suggested by Ambjorn et al. in their analysis of the spectral dimension in CDT [20],

$$D_s(\sigma) = a - \frac{b}{c + \sigma} \tag{18}$$

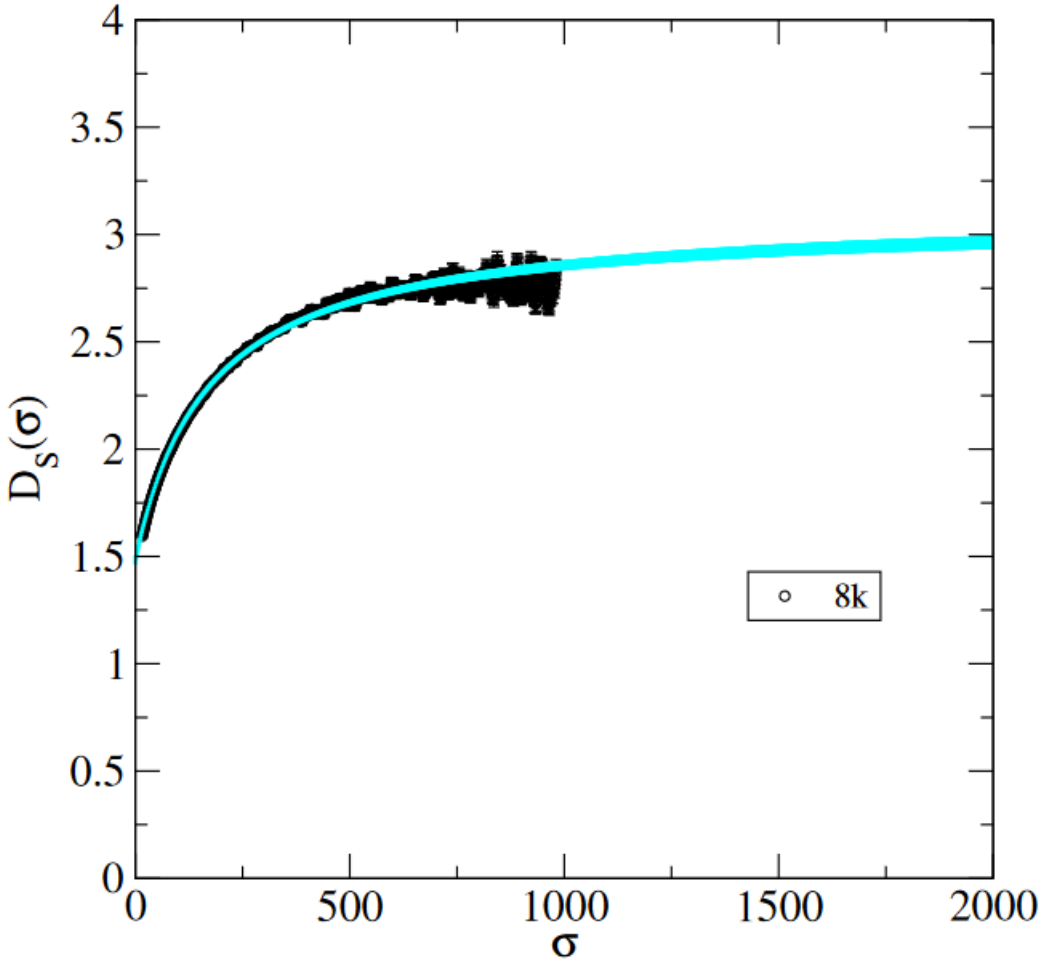

Figure 13: The spectral dimension as a function of distance scale probed in black, as well as the fit suggested by Ambjorn et al. in cyan.

where a, b, and c are free parameters. Table 2 gives the results for the fits to every available ensemble of this quantity. All errors are purely statistical.

Care must be taken in selecting the range, σ_{min} to σ_{max}, in which to compute the fit. If σ_{min} is taken to be too small, discretization effects will contaminate the fit, but we'd like σ_{min} to be as low as possible to include the maximum amount of data. In practice, a value of $\sigma_{min} \approx 60 - 100$ is sufficient to reduce this contamination to acceptable levels, and is supported by a study of the spectral dimension in the branched polymer phase where the answer is known. [18]. If σ_{max} is taken to be too large the fit will include finite size effects

Volume	β	$\sigma_{min} - \sigma_{max}$	$D_S(0)$	$D_S(\infty)$	$\chi^2/d.o.f.$
16k	0	61-611	1.484(37)	3.30(12)	0.92
8k	0	61-611	1.484(21)	3.090(41)	1.25
4k	0	61-556	1.464(49)	2.809(15)	1.12
4k	1.5	61-138	1.64(26)	2.655(93)	1.60
8k	-0.8	105-831	1.445(16)	2.75(11)	1.14

Table 2: The results for the spectral dimension at 0 and infinity from the fits to Eq.(19)

which cause the lattice data to stop its monotonic increase and turn over. It would then be impossible for the ansatz in Eq.(18) to describe the data.

The plot of the $\beta = 0$, 8k ensemble suggests that $D_S(\infty) = 2.7$-3.3 with errors of a few percent, clearly inconsistent with 4. However, each of the ensembles is of finite volume and non-zero lattice spacing, so there is the possibility that the deviation from 4 is due to finite-volume and discretization effects. This suggests that to obtain the value of $D_S(\infty)$, we must take the infinite-volume and continuum limit. We do this by determining $D_S(\infty)$ for each ensemble, and then fitting to the function

$$D_{S\infty}(V, a) = c_0 + c_1 \frac{1}{V} + c_2 a^2 \tag{19}$$

where V is the physical volume of the ensemble, the number of 4-simplices multipled by the lattice spacing to the fourth power, a is the lattice spacing, and the c_i are fit parameters. The lattice spacing scaling is assumed to be dependent on a^2 because diffeomorphism invariance forbids an odd power term, and that some lattice spacing dependence seems to be present means that the power cannot be 0. Note that in doing this procedure, we tacitly assume that the general coordinate invariance symmetry broken by the lattice regulator has been restored by correctly tuning β, on which more below.

Figure 14 shows the extrapolation of $D_S(\infty)$ for all but the finest ensembles. Note that

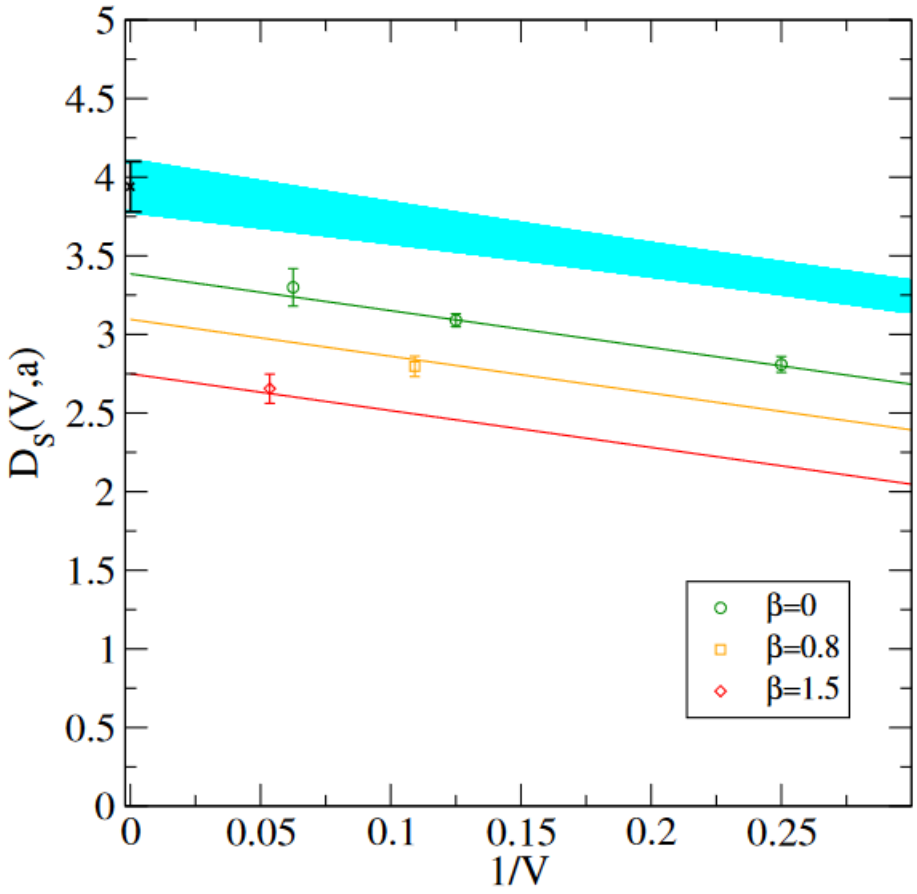

Figure 14: The spectral dimension at large distances $D_S(\infty)$ for many different ensembles, and the extrapolation to infinite volume and zero lattice spacing in cyan. Especially fine ensembles are excluded

each value of β is associated with a particular lattice spacing. Specifically, the lattice spacing shrinks as β is taken to smaller values. The blue bar represents the range of possible extrapolations, and gives a value in the infinite volume, continuum limit of $D_S(\infty) = 3.94 \pm 0.16$, where the error is purely statistical. The quality of the fit is quite good, with a $\chi^2/d.o.f.$ of 0.52.

The finer ensembles can be added to the data, but this requires an alteration to the ansatz. These fine ensembles have very small physical volumes which appear to favor the inclusion of a $\frac{1}{V^2}$ term to the fit function in Eq.(19). This extrapolation is shown in Figure

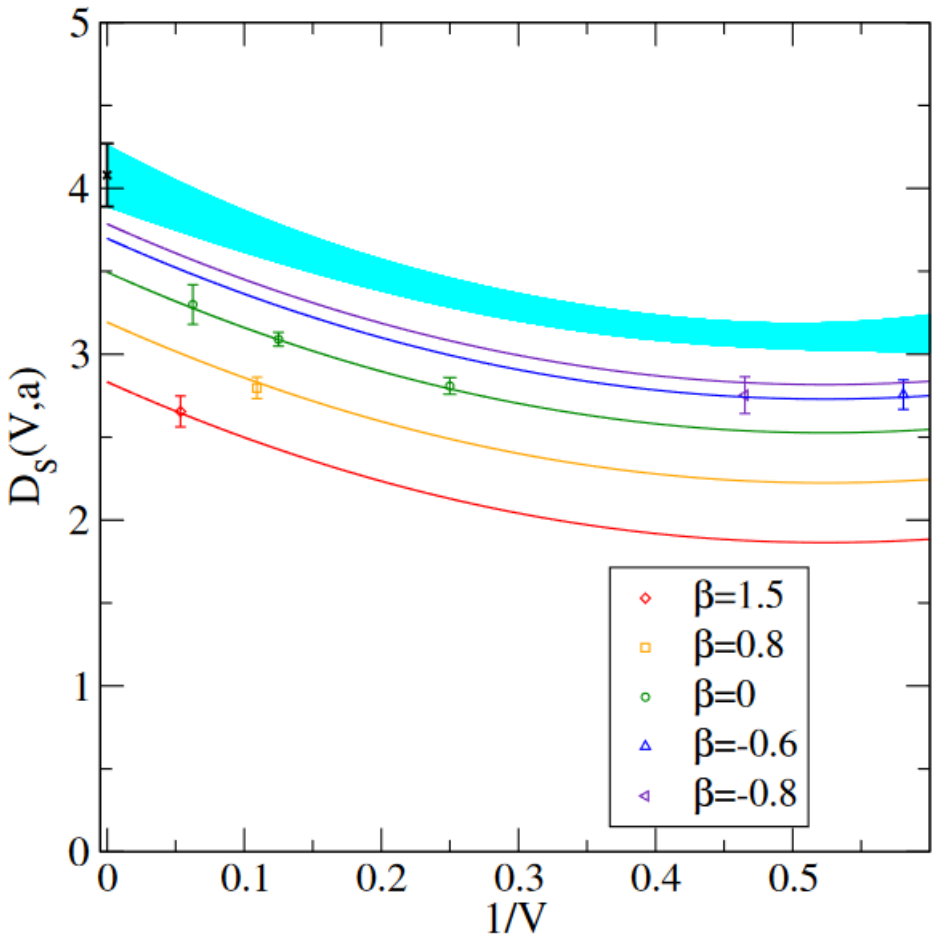

Figure 15: The spectral dimension at large distances $D_S(\infty)$ for many different ensembles, and the extrapolation to infinite volume and zero lattice spacing in cyan. The especially fine ensembles are included, and so a $\frac{1}{V^2}$ term is included in the fit function.

15. The fit gives a value of $D_S(\infty) = 4.08 \pm 0.19$ and the quality of the fit is again excellent; $\chi^2/d.o.f. = 0.32$. If the $\frac{1}{V^2}$ term is not included, the fit is considerably worse.

The systematic error associated with this extrapolation is difficult to measure. An estimate can be gleaned from the scatter of the results for $D_S(\infty)$ by the different fits, but this does not fully account for the dependence of the extrapolation on the choice of the fit ansatz. To really get a handle on the systematics, more data, specifically from lattices with larger volumes and finer lattice spacing, is needed. However, the work done here suggests

that it is possible to recover the value of 4 for the long distance spectral dimension for EDT.

2.6.3 Entropy Scaling of Black Holes

An argument was made by Banks [37] against the notion of gravity being asymptotically safe, since the resultant entropy scaling of black holes would be inconsistent with the scaling determined in holography.

A renormalizable quantum field theory is a perturbation of a conformal field theory by relevant operators, and so the density of states for the renormalizable theory must be the same as that of a conformal theory. For the conformal theory, the scaling of energy and entropy must be extensive in the lattice volume, and since no other dimensionful scales other than temperature exist for a finite temperature conformal field theory, it must be that

$$S \sim (RT)^{d-1}. \qquad E \sim R^{d-1}T^d \tag{20}$$

with R the radius of the spatial volume, T the temperature, and d the dimension of space-time. It follows that, for a renormalizable theory, entropy must scale with energy according to

$$S \sim E^{\frac{d-1}{d}} \tag{21}$$

For gravity, it is argued that black holes dominate for high energies. The Bekenstein-Hawking entropy formula tell us that in a d-dimensional space-time, the entropy scaling of a black hole with energy in the Schwarzschild solution on an asymptotically flat space-time is

$$S \sim E^{\frac{d-2}{d-3}} \tag{22}$$

Comparing with Eq.(21), we see that for d=4, these results do not agree. However, since the theory is formulated on a fractal space-time, the spectral dimension is what is needed in equations of state [38] and for a black hole [39]. Hence, the value of $D_S(0)$ is what should be used to compare the entropy scaling.

Table 2 includes a column for $D_S(0)$. We must perform the same extrapolation to infinite volume and the continuum as was done for $D_S(\infty)$. With the finest lattices excluded and no $\frac{1}{V^2}$ term in the extrapolation, $D_S(0) = 1.44 \pm 0.19$ with $\chi^2/d.o.f. = 0.17$, plotted in figure 16. With the finest lattices included and the $\frac{1}{V^2}$ term restored to the fit function, $D_S(0) = 1.48 \pm 0.11$ with $\chi^2/d.o.f. = 0.11$, plotted in figure 17. The same caveat about the lack of control for systematic errors remains, but the data suggests that $D_S(0) \sim 1.5$, and disfavor 2, which previous studies suggested.

The value of 1.5 is the unique value such that the entropy scaling in Eq.(21) and Eq.(22) agree. The tension between holography and renormalized field theory is resolved, provided this result holds up. The fact that the field theory gives exactly the right dimension needed for this scaling to match turns Banks argument from one against asymptotic safety into an argument for it.

3 Running of the Couplings

The lattice implementation has three parameters, β, κ_2, and κ_4. If asymptotic safety is realized for gravity, then as the continuum limit is approached, the relevant couplings should approach fixed point values with a UV critical surface of some finite dimensionality. Verifying that this is the case is essential, and so the parameters of the lattice implementation must be analyzed for the fixed point behavior, if it exists. The dimensionality of the UV critical surfaces tells one how many dimensionful parameters the model requires as inputs

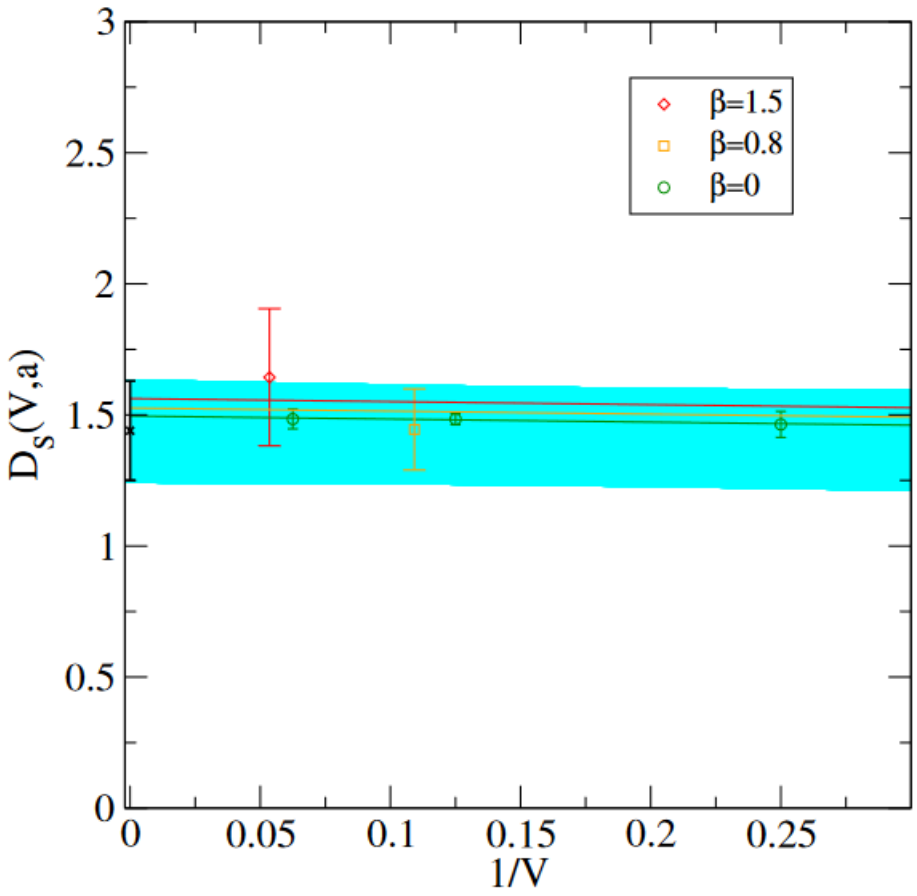

Figure 16: The spectral dimension at short distances $D_S(0)$ for many different ensembles, and the extrapolation to infinite volume and zero lattice spacing in cyan. The especially fine ensembles are excluded.

from experiments to make predictions, and so is of great importance.

We argue that of the three parameters, only two combinations of them are relevant, i.e. contribute to on-shell observables. However, one of them is needed to restore a continuum symmetry that is broken by the regulator and must be fine-tuned. In the case that the symmetry is an exact one of the quantum theory, we would expect only one more parameter in the lattice action compared to the continuum theory. The correct continuum physics is recovered and the UV critical surface of the symmetry-restored theory appears to be 1-dimensional.

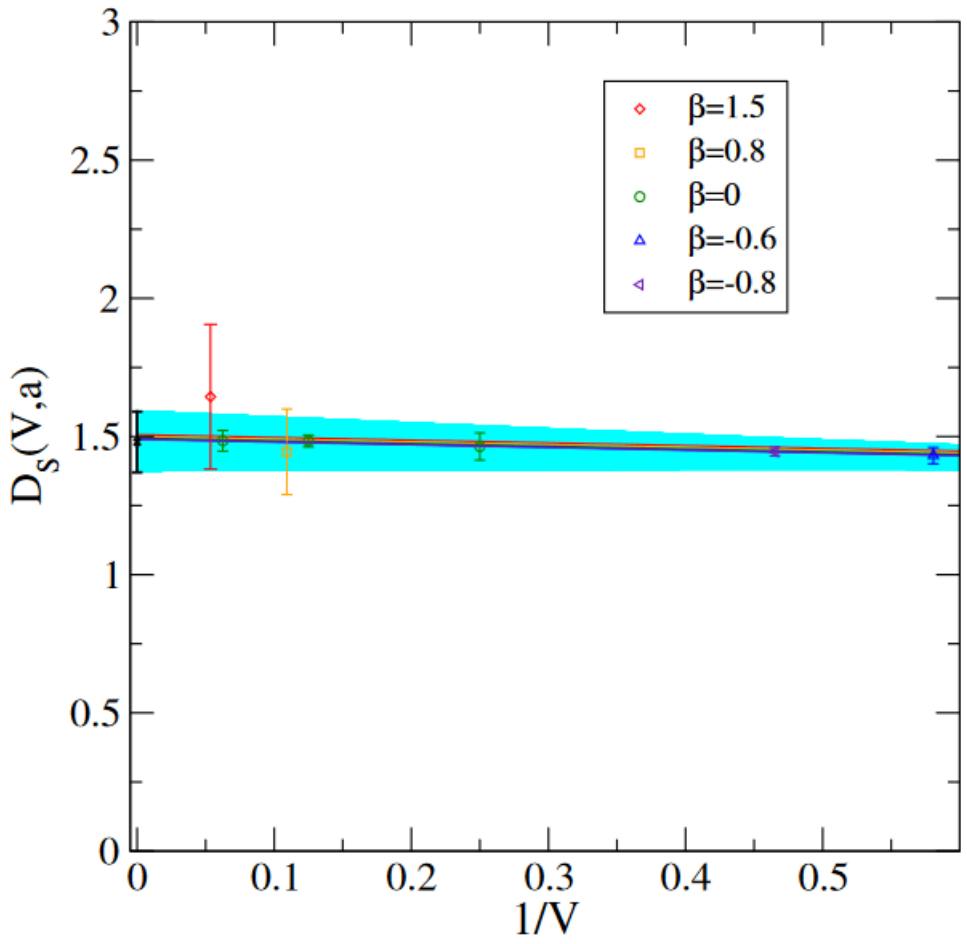

Figure 17: The spectral dimension at short distances $D_S(0)$ for many different ensembles, and the extrapolation to infinite volume and zero lattice spacing in cyan. The especially fine ensembles are included, necessitating the inclusion of a $\frac{1}{V^2}$ term in the fit function.

3.1 Redundant Operators

We can invert the defintions of κ_2 and κ_4 to find G and Λ in terms of lattice parameters:

$$G = \frac{\sqrt{3}}{16}\frac{1}{\kappa_2} \qquad \Lambda = 48\pi\sqrt{\frac{3}{5}\frac{\kappa_4}{\kappa_2}} - 48\ \arccos(1/4)\sqrt{15} \tag{23}$$

where κ_2 is an input to the simulations, while κ_4 is determined from the tuning of the volume. As such, we know explicitly how G runs as a function of κ_2, and it asymptotes to 0 for large values of κ_2. On the other hand, Λ must be measured from the simulations. As κ_2

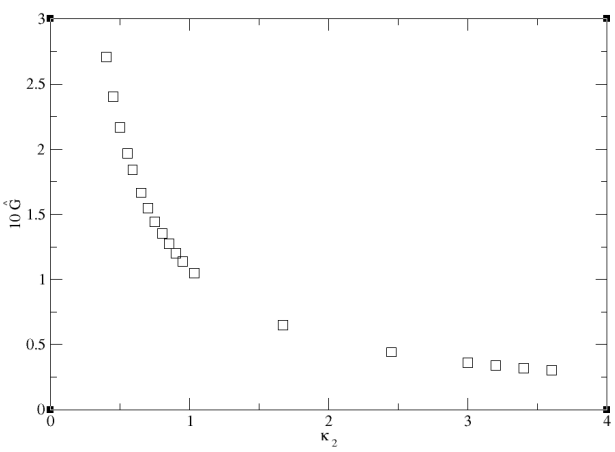

(a) $10\hat{G}$ in lattice units as a function of κ_2

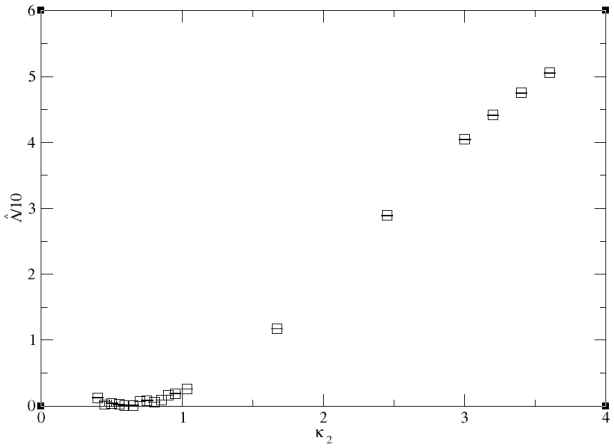

(b) $\hat{\Lambda}/10$ in lattice units as a function of κ_2

increases, the lattice spacing decreases. It is then interesting to examine how the couplings run for large κ_2 in order to investigate the UV fixed point.

It is convenient to define the dimensionless Newton's Constant and cosmological constant, $\hat{G}$ and $\hat{\Lambda}$:

$$\hat{G} = G/a^2, \qquad \hat{\Lambda} = \Lambda a^2 \tag{24}$$

since it is the *dimensionless* couplings that must approach a UV fixed point for an asymptotically safe theory. Plots of $\hat{G}$ and $\hat{\Lambda}$ are given in Figure 18a and Figure 18b respectively, where a rescaling by a factor of 10 has been done for later convenience. We point out again that κ_2 is used as a proxy for lattice spacing. For large κ_2, $\hat{\Lambda}$ does not appear to approach a fixed point value, unlike $\hat{G}$. If this result held, it would spell disaster for the idea of gravity being asymptotically safe. However, this can be avoided if $\hat{\Lambda}$ is *redundant* (or if this coupling has a redundant multiplicative factor), i.e. that on-shell reaction rates do not depend on it, as it can be treated as a field redefinition. A redundant coupling is not required to approach a UV fixed point, even in an asymptotically safe theory

There is a standard test for the redundancy of a coupling [4]. If, for a coupling γ, the

partial derivative of the Lagrangian with respect to that parameter $\frac{\partial \mathcal{L}}{\partial \gamma}$ vanishes or is a total derivative under the Euler-Lagrange equations of motion, then γ is redundant. The associated operator must also be an eigenoperator of the theory. Since this depends on the running of the couplings near the fixed point, and thus on the dynamics of the theory, this is harder to test.

To examine this for the Einstein-Hilbert action, we rewrite the action as

$$\mathcal{L} = \frac{1}{16\pi G}(R - 2\Lambda) \rightarrow \mathcal{L} = \frac{\omega}{16\pi}(R - 2\omega\Lambda') \tag{25}$$

where $\omega = \frac{1}{G}$ and $\Lambda' = G\Lambda$. Performing the test on the parameter ω we find that

$$\frac{\partial \mathcal{L}}{\partial \omega} = \frac{1}{16\pi}(R - 4\omega\Lambda') \tag{26}$$

Under the equations of motion, $R = 4\Lambda$, so the term in parenthesis, $R - 4\omega\Lambda'$ is equal to 0, and so

$$\frac{\partial \mathcal{L}}{\partial \omega} = 0 \tag{27}$$

Hence, $\omega = 1/G$ could be redundant. The remaining coupling, $\Lambda' = G\Lambda$ could be relevant, as well as β. That $\hat{\Lambda}$ does not converge to a fixed point is no longer a concern, as it is the combination $\hat{G}\hat{\Lambda} = G\Lambda$ that might be relevant.

3.2 Restoring General Coordinate Invariance

The above argument that only $G\Lambda$ is relevant holds only if general coordinate invariance is respected, so that the field redefinition that leads to the redundancy of the couplings can be performed. However, the lattice regulator appears to break this symmetry. Before the

above argument can be followed through, this broken symmetry must be restored by the fine-tuning of a free parameter. This is the justification for the introduction of the measure term β; it is the coefficient of the needed term to restore the symmetry.

The introduction of β however has a side effect. The renormaliziation of β also renormalizes the cosmoglogical constant. Since the running of β is unphysical, so too is the renormalization of Λ by β. This unphysical contribution to Λ, and thereby $G\Lambda$, must be subtracted to obtain the correct running, or more practically, β must be tuned to the correct value so that the symmetry is restored and the unphysical contribution is not present.

In this situation, one expects that the running of the bare couplings is modified when the regulator breaks a symmetry. To recover the running in the symmetry preserving theory generically requires a subtraction. This type of subtraction is familiar in other lattice theories, such as the running of quark masses in QCD with Wilson fermions. However, it remains to specify what the subtraction criterion is in our case.

Previous results suggest that, at long distances, the geometries are de Sitter like, and as in classical general relativity with a positive cosmological constant, the cosmological constant should set the size of the Universe. On the lattice, the lattice volume sets the IR cutoff for Λ, $\Lambda \propto \frac{1}{\sqrt{V_r}}$, and so as we take the large volume limit, Λ goes to very small values. In order that there be a wide range of scales behaving like de Sitter space, this running must be a power law that is quadratic or greater in the renormalization scale so that the effective cosmological constant vanishes fast enough. This leads to the prediction for $G\Lambda$ that both its value and its derivative should be simultaneously 0 in the IR.

A plot of $G\Lambda$ for several values of β is shown in figure 19. For $\beta = -0.8$ or greater, $G\Lambda$ diverges monotonically to ∞ in the IR. For values of $\beta = -1$ and lower, $G\Lambda$ diverges

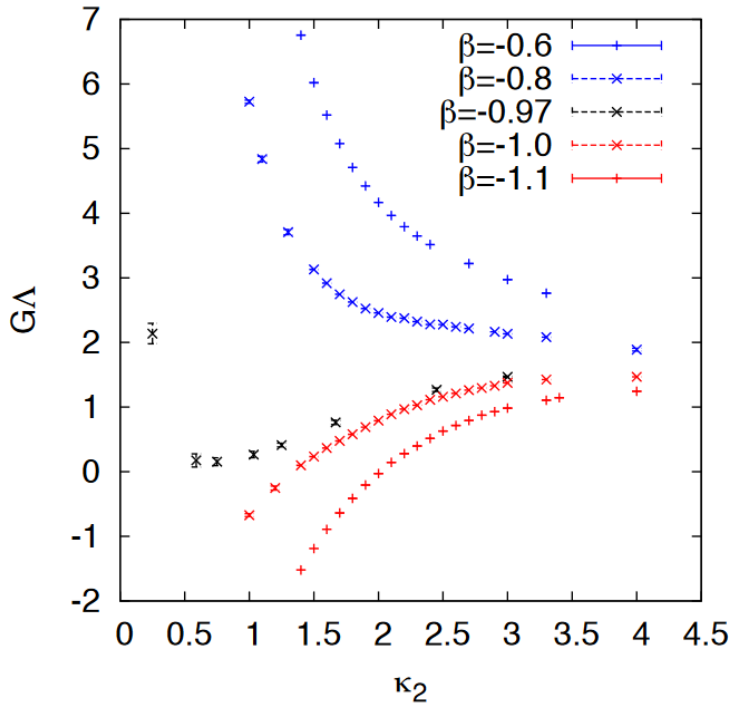

Figure 19: GΛ as a function of κ_2 for many different values of β.

monotonically to $-\infty$. However, between $\beta = -0.8$ and $\beta \approx -1$, $G\Lambda$ drops down to a local minimum before diverging. By selecting the right value of β, this minimum can be made to coincide with $G\Lambda = 0$. Working under the assumption that in the symmetry-restored theory, β shouldn't run, we try to find a fixed value of β for which this condition on the running of $G\Lambda$ is satisfied.

This is our subtraction criterion. β shall be tuned so that the minimum of $G\Lambda$ has a local minimum that coincides with 0. It's a strong consistency check that not only does this happen at all, but does so far into the IR. There is a volume dependence, but $\beta \approx -0.97$ appears to be around the correct value.

Another consistency check is to confirm that the subtracted value of β is consistent with the continuum value of β one gets by following the phase transition line to what appears to be a horizontal asymptote. The phase diagram in figure 1 suggests that the continuum value

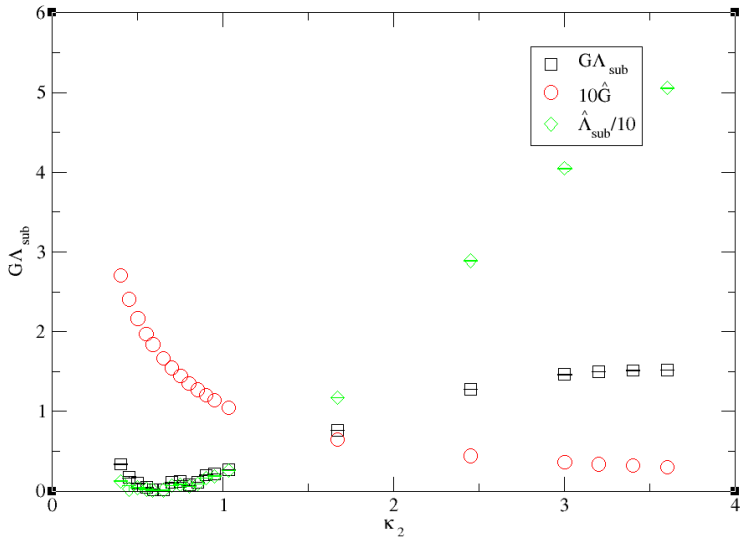

Figure 20: $G\Lambda_{sub}$, $\hat{\Lambda}_{sub}/10$, and $10\hat{G}$ plotted together as a function of κ_2.

for β, though the precise value cannot be obtained as of yet, is approximately -1, which is consistent with the tuned β needed to restore the symmetry.

Figure 20 shows $G\Lambda$, $\hat{G}$, and $\hat{\Lambda}$ plotted as functions of κ_2 together. $G\Lambda$ appears to be leveling off to an asymptote at some constant value. This is the expected behavior for a relevant coupling as it approaches a UV fixed point.

3.3 Dimension of the UV critical surface

Asymptotic safety posits that in the UV, relevant couplings should approach fixed point values. The preceding arguments lead us to conclude that only $G\Lambda$ is relevant, rather than G and Λ separately. β is a non-physical coupling put in place to be fine tuned to restore general coordinate invariance symmetry, which the lattice regulator breaks. A subtraction is generally necessary when the regulator breaks a symmetry. After introducing a plausible subtraction condition, we find that $G\Lambda$ runs exactly the way that one would expect for asymptotic safety, though $\hat{\Lambda}$ does not.

This provides evidence that in the target continuum theory theory, there is only a single relevant coupling, and the UV critical surface is 1-dimensional. In that case the theory is maximally predictive; only a single dimensionful quantity needs to be determined in order to set the scale, and then all other quantities become predictions. If this continues to hold with matter fields included, many interesting quantities, including the cosmological constant, could potentially be predicted from first principles.

4 Curvature Correlators

The simplest type of object to calculate in a quantum field theory is the two point correlation function $\langle AB \rangle (r)$, where A and B are observables and r is the geodesic distance between them. This tells us about how the fields of the theory propagate. For gravity, a natural choice for an observable is the scalar curvature R, the correlation function of which tells us how gravity acts at a distance and can potentially be used to extract couplings in the low energy effective theory.

In EDT, curvature is defined on the $(d-2)$-dimensional objects, so in 4d this is the triangles. Using parallel transport of vectors, it is found to depend on two geometric properties. The first is the deficit angle $\delta(T) = 2\pi - \arccos(1/\mathrm{d})\mathcal{O}(T)$, which is the amount of angle around triangle T that is missing or added from flat space. The second is the 4-volume associated with triangle T, $V(T)$. Since all structures are regular, each triangle should receive an equal amount of volume in each simplex. As there are 10 triangle to a simplex, each triangle should receive $\frac{1}{10}$ of a single simplex volume for each simplex it is a subsimplex of, so that $V(T) = \frac{1}{10}\frac{\sqrt{5}}{96}\mathcal{O}(T)$. Written explicitly, the curvature of triangle T is

$$R(T) = 480\sqrt{\frac{3}{5}}\left(\frac{2\pi}{\mathcal{O}(T)} - \arccos(1/4)\right) \tag{28}$$

Since the EDT formulation does not utilize a coordinate system, thought must be given to how the distance between a pair of triangles is to be defined. The most straightforward would be to declare neighboring triangles as being one geodesic distance apart, and those that require an intermediate triangle as two distances apart, and so on. There are at least two definitions of neighboring triangle that may be used [40]; triangles may be defined to be neighbors if they share a side, or if they both share a side and are subsimplices of at least one common simplex. In the continuum, the choice of discretization should not matter, and so which definition one uses is a matter of convenience. However the less restrictive definition

of requiring only a common side results in a very short number of hops to traverse the entire lattice, and so it is difficult to probe distance dependence. The latter definition requiring a common side and common 4-simplex will be used in the rest of this work. This follows the definition of distance adopted by de Bakker and Smit [40].

While curvature is defined for triangles, it can also be defined for 4-simplices in a simple way. Define the curvature of a simplex S to be the average of the curvatures of each of its triangles

$$R(S) = \frac{1}{10} \sum_{T \in S} R(T) \tag{29}$$

Neighboring simplices are defined simply as those that share a common tetrahedron.

In what follows, an analysis will be done for both the triangle and 4-simplex implementations of the two-point function $\langle RR \rangle (r)$. If the same results are found for both approaches, it will provide evidence that the behavior is universal, rather than a quirk of the particular choice of discretization of curvature.

The correlators are computed for the ensembles that were tuned to the phase transition line according to the prescription in Section 2. In principle, one could draw only a single triangle pair from each configuration, but even for long running ensembles this will result in very low statistics. Instead, we take many pairs from each configuration and average them, and then we take the ensemble average [40].

The distortion of our geometries at long distances for coarse couplings presents an added complication. In the continuum this effect appears to vanish, it is likely non-physical, and correlators sourced from this region likely contaminate the results. To avoid this, source

triangles are biased to come from within the bulk universe. This is accomplished as in the analysis of the spectral dimension. We pick a single source triangle at random to be the origin and make a list of all triangles a distance r from this source triangle. A distance we call r_{max} will have the largest number of triangles at that distance, and these triangles are more likely to be in the bulk universe. We use these triangles as the sources for our correlators. This procedure is also being used in an investigation of matter fields [45] [46].

4.1 Unsubtracted Correlation Functions

The above discussion necessitates that, for each configuration in an ensemble, the following be calculated [40]

$$\langle RR \rangle (r)_{conf} = \frac{1}{N_x} \sum_{x \in source} \frac{1}{N_{yx}} \sum_{y} R(x)R(y)\delta_{d(x,y),r} \tag{30}$$

The sum in x is over triangles in the list of source triangles in the bulk universe, and $d(x, y)$ gives the geodesic distance between the triangles at x and y. N_x is the number of source triangles, and N_{yx} is the number of triangles a distance r away from source triangle x. The delta function $\delta_{d(x,y),r}$ ensures that the triangles are a distance r apart. This is calculated for each configuration, and then the ensemble average over configurations is taken.

The correlator for triangles for the 16k, $\beta = 0$ ensemble is plotted in Figure 21. The unphysical behavior is apparent: the correlator does not asymptote to a constant at long distance. The cause of this unphysical behavior is an over counting of geometry [41]. In Eq.(30), curvature is obviously a function of geometry. However, the separator $\delta_{d(x,y),r}$, is also a function of geometry, since the probability of two points being separated by a distance r depends on the geometry. This over counting can be readily seen by plotting the correlator with 1 at the origin

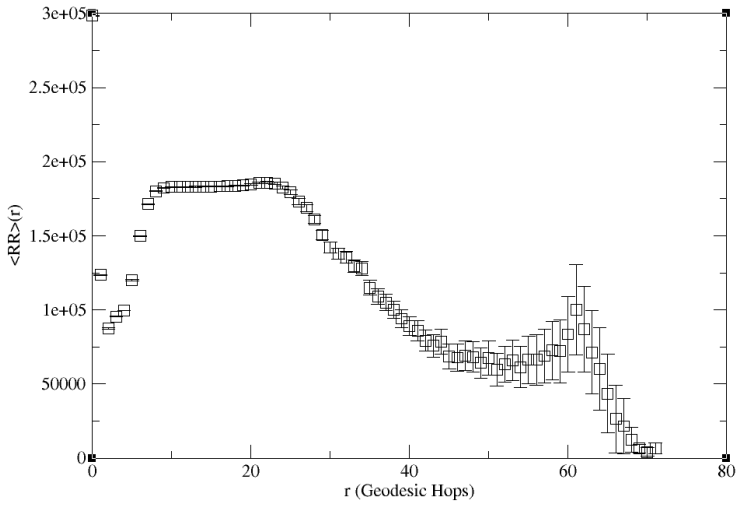

Figure 21: The correlator as defined in Eq.(30) for the 16k $\beta = 0$ ensemble.

$$\langle 1R \rangle (r)_{conf} = \frac{1}{N_x} \sum_{x \in source} \frac{1}{N_{yx}} \sum_{y} 1R(y) \delta_{d(x,y),r} \tag{31}$$

There should be no correlation, yet the plot in figure 22 shows a clear, non-vanishing correlation. This *disconnected* correlation must be removed to obtain the correct physics. Suggestively, the two correlators appear to have a very similar form, but with different magnitudes.

4.2 Connected Correlators

A simple approach to subtract the disconnected contributions to the correlator was proposed by de Baker and Smit [40], where one simply squares the disconnected correlator in Eq. (31) and subtracts it from the correlator in Eq.(30). An example of this is plotted in figure 23. The results seem quite good; it appears that there is an asymptote for large distances, even though it's not at 0.

However, a further refinement was proposed by Ambjorn et al. [42] Start by defining the

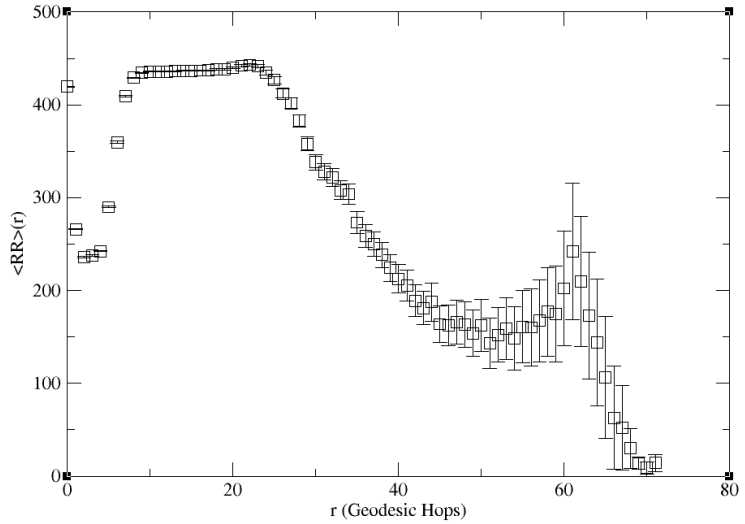

Figure 22: The correlator defined in (31), which should have no measured correlation.

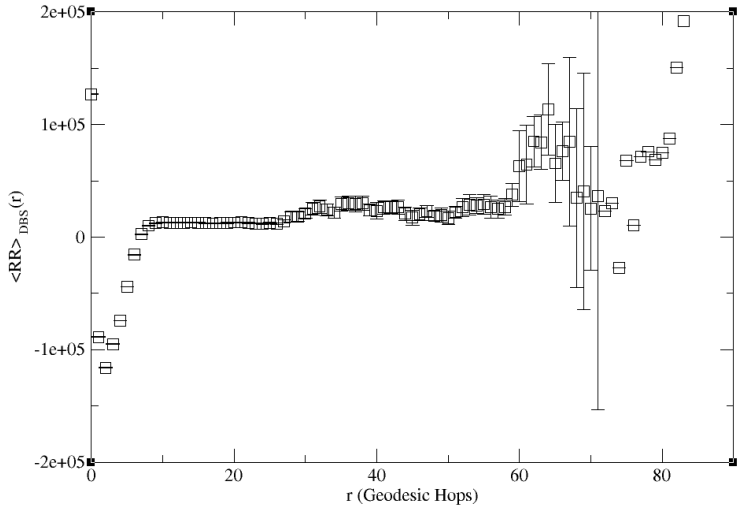

Figure 23: The modified correlator proposed by de Baker and Smit.

unnormalized correlation function

$$G^{AB} = \sum_{x,y} A(x)B(y)\delta_{r,d(x,y)} \tag{32}$$

where A and B can be any operators. Specifically, there are three unnormalized correlators that we need, G^{11}, G^{1R}, and G^{RR}.

Ambjorn's refinement was to assume the ansatz

$$G^{1R}(r) = A\ G^{11}(r+\delta) \tag{33}$$

for constants A and δ, which are obtained by fitting $G^{1R}(r)$ to $G^{11}(r)$ measured from the ensemble, with a cubic spline used to evaluate $G^{11}(r)$ for non-integer r. This ansatz was determined by studying how correlations can be factorized for large r and all r for many different systems, including 2d gravity where analytic results can be compared against. Then, the connected correlator is

$$\langle RR \rangle_c (r) = \frac{G^{RR}(r) - A^2 G^{11}(r+2\delta)}{G^{11}(r)} \tag{34}$$

The connected correlators for the triangle approach are shown in Figures 24-29, and for simplices in Figures 30-35.

A few features are immediately striking. First is the very large errors for large values of r. The proposed explanation is that this is caused by contamination by the baby universe tails, which should become dominant at large distances. Since the source triangles and simplices are biased to be in the bulk universe, distant triangles and simplices are more likely to be in the baby universe tails, which are unphysical. We thus focus on the behavior of the subtracted correlators at shorter distances.

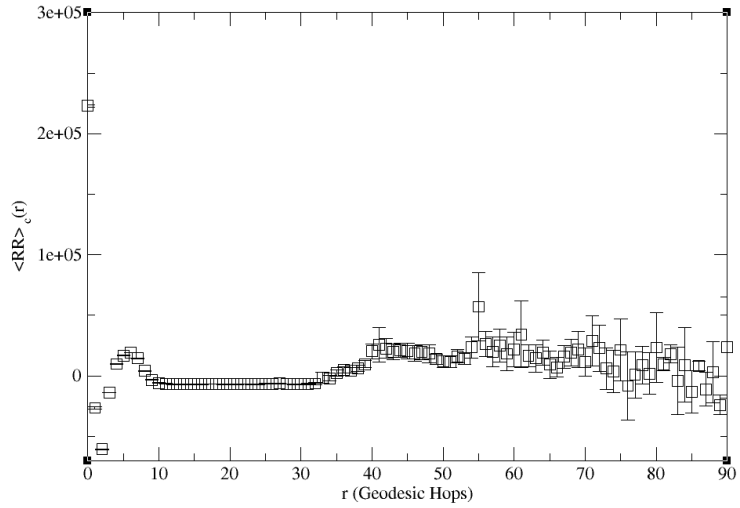

Figure 24: The connected correlator for the 32k $\beta = 0$ ensemble in the triangle approach.

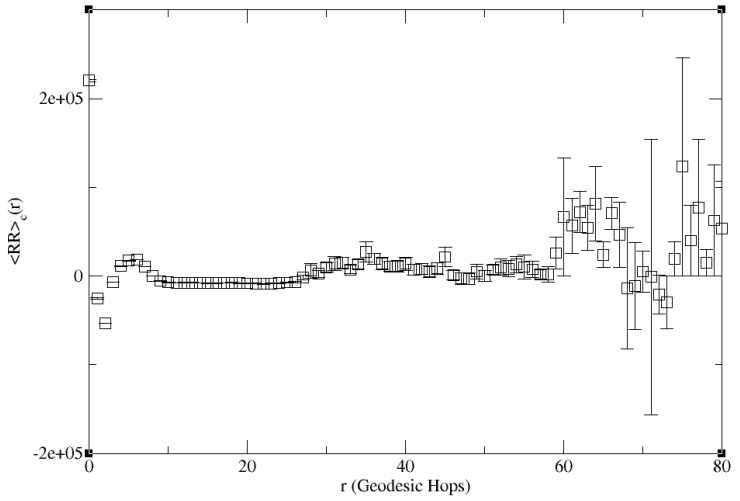

Figure 25: The connected correlator for the 16k $\beta = 0$ ensemble in the triangle approach.

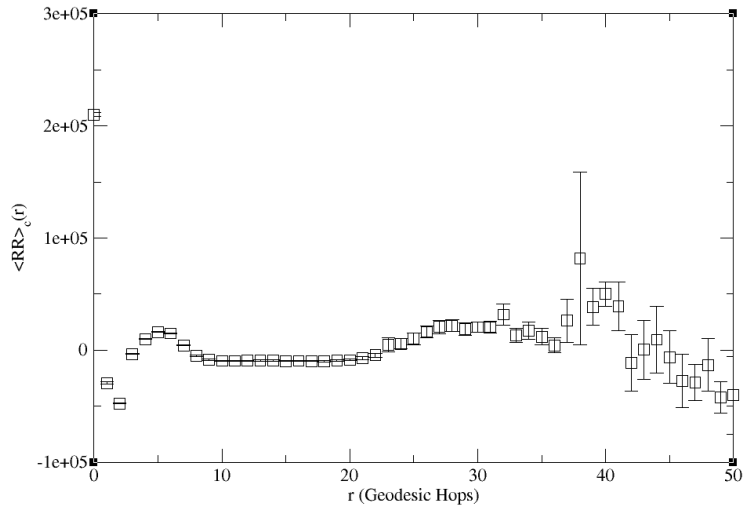

Figure 26: The connected correlator for the 8k $\beta = 0$ ensemble in the triangle approach.

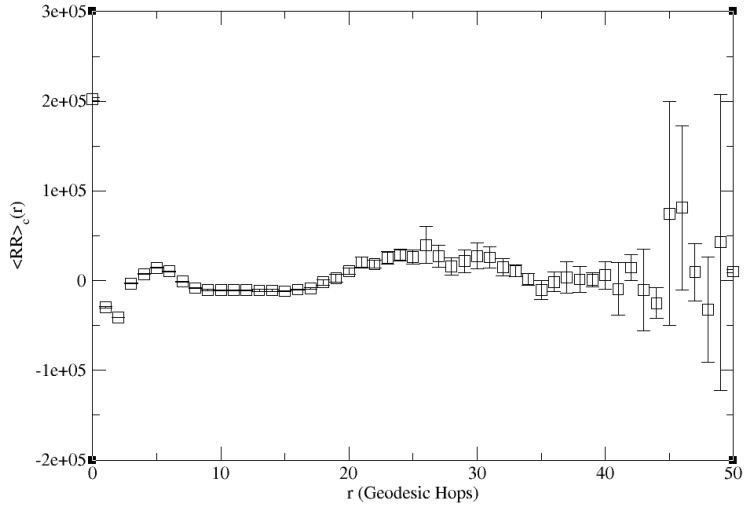

Figure 27: The connected correlator for the 4k $\beta = 0$ ensemble in the triangle approach.

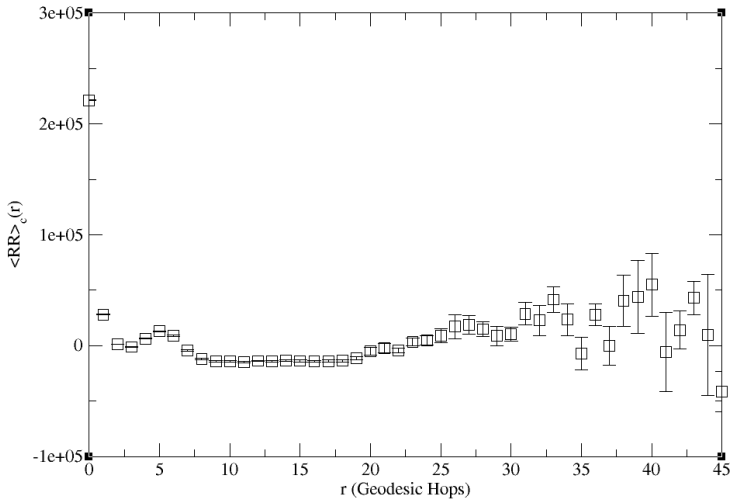

Figure 28: The connected correlator for the 4k $\beta = 1.5$ ensemble in the triangle approach.

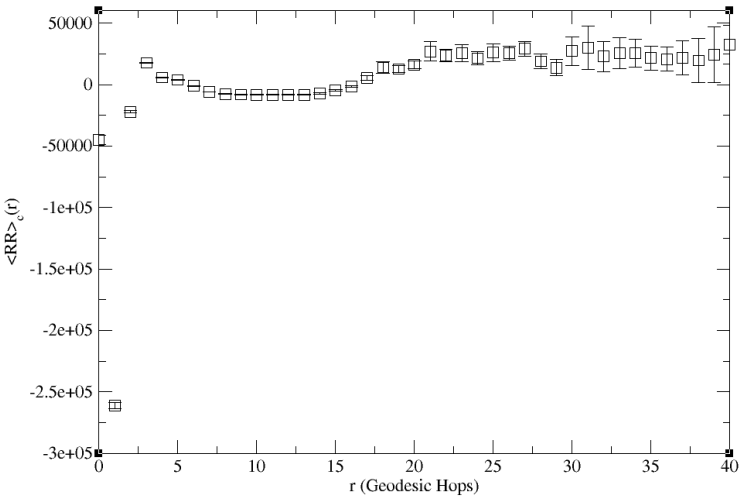

Figure 29: The connected correlator for the 8k $\beta = -0.8$ ensemble in the triangle approach.

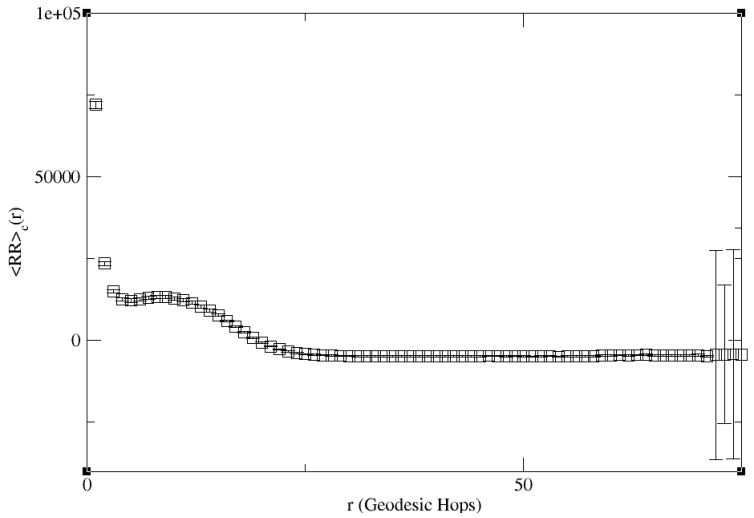

Figure 30: The connected correlator for the 32k $\beta = 0$ ensemble in the simplex approach.

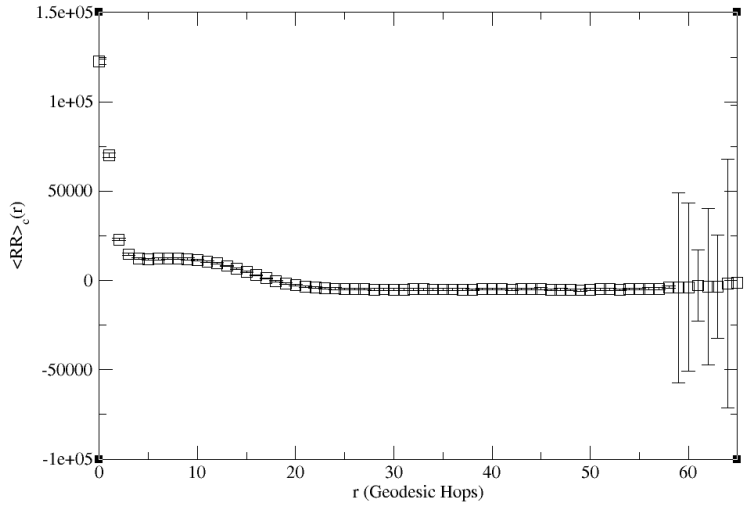

Figure 31: The connected correlator for the 16k $\beta = 0$ ensemble in the simplex approach.

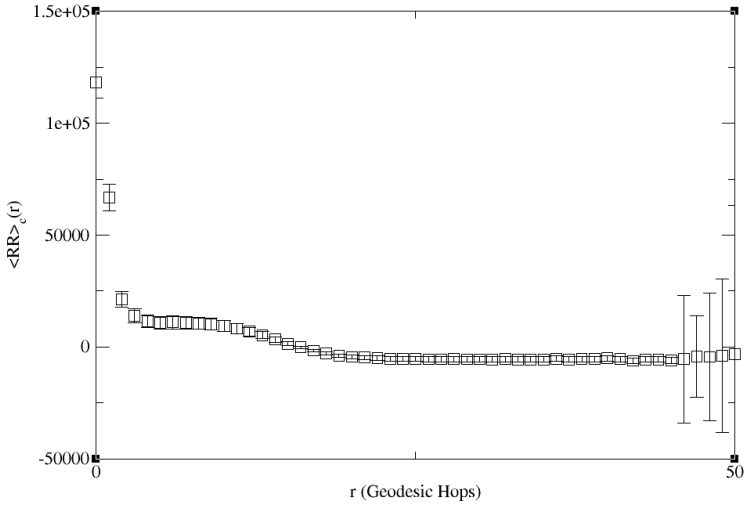

Figure 32: The connected correlator for the 8k $\beta = 0$ ensemble in the simplex approach.

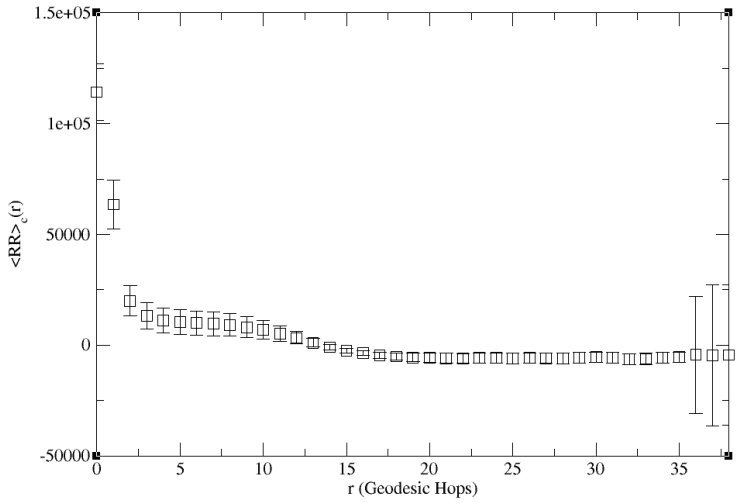

Figure 33: The connected correlator for the 4k $\beta = 0$ ensemble in the simplex approach.

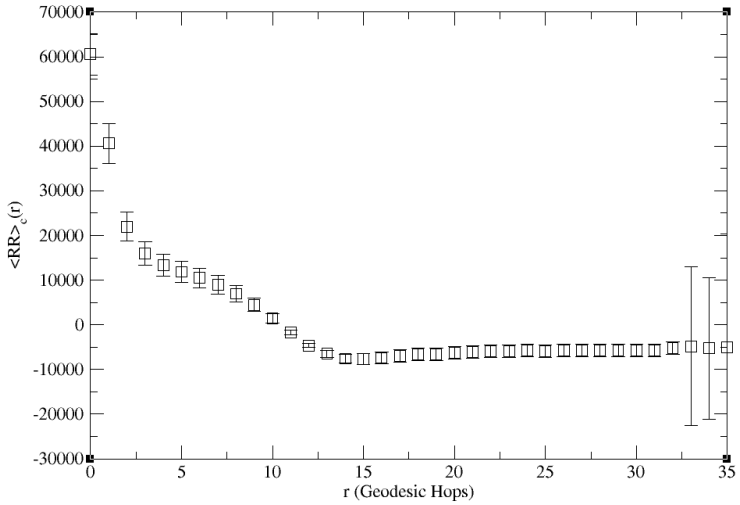

Figure 34: The connected correlator for the 4k $\beta = 1.5$ ensemble in the simplex approach.

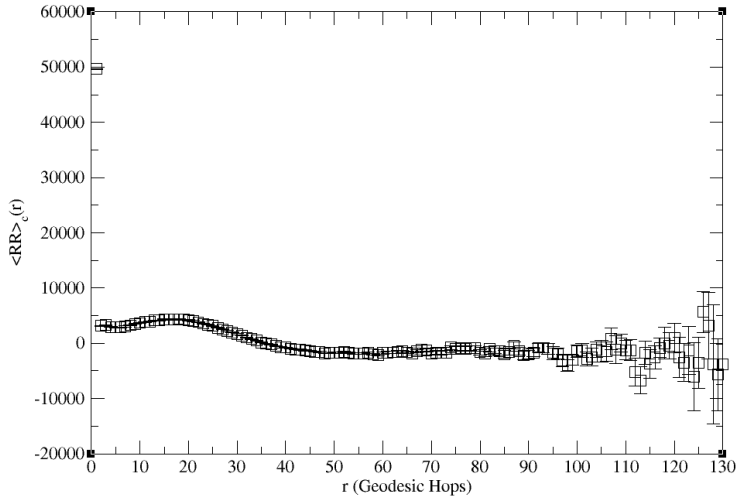

Figure 35: The connected correlator for the 8k $\beta = -0.8$ ensemble in the simplex approach.

Next is the asymptotic behavior. For large r, we observe an asymptote that continues until the effects of the baby universe tails become dominant, but the asymptotes are at negative values, presenting issues for unitarity. We conjecture that this is a discretization effect. For the $\beta = 0$ ensembles in figures 24-27 and 30-33, we see that as the volume increases, the asymptote increases to a smaller negative value at infinite volume. This raises the hope that if the continuum limit were also taken, the asymptote would vanish. However, the asymptotes are dimensionful quantities with units of inverse mass to the fourth power. To compare the asymptotes, these must be made dimensionless by dividing by a^4 where a is the relative lattice spacing. This would drop the finest lattice spacing asymptote to larger negative numbers and the coarsest lattice spacing asymptotes to smaller negative numbers, the opposite of the expected trend. It could be that the asymptotes at the finer lattice spacing decreases faster with decreasing volume than the coarser ones, but verifying this would require ensembles at the same fine lattice spacing but additional physical volumes. We do not at present have such ensembles available, but the volume trend at fixed lattice spacing suggests that this may be possible. We assume from this point that this is the case, but admit that this must be verified in a future work.

The simplex correlator for the $\beta = 1.5$ ensemble appears to be an outlier. There is a weird "bump" prior to the asymptote that is not present in any other ensemble, which can be seen in the zoomed in view in Figure 36. That this is the coarsest lattice would suggest that a deviation could be a discretization error, but this bump does not appear to be present in the triangle correlator from the same ensemble. This could be explained by the fact that the simplex curvature is more smeared than the triangle curvature, which leads to larger discretization effects. This leads us to exclude this ensemble from the subsequent analysis for the simplex definition of curvature.

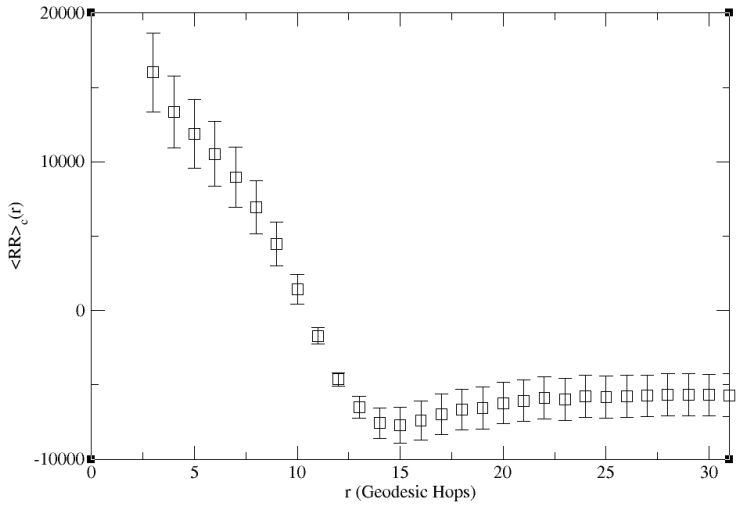

Figure 36: The correlator for the 4k $\beta = 1.5$ ensemble with the simplex discretization, zoomed in to highlight the "bump" that is absent for other ensembles.

4.3 Power Law

For small values of r where the distance scales are close to the lattice spacing, lattice artifacts should wash out the physics, and give non-universal results [43]. On the other hand, for very large values of r so that we approach the edge of the lattice, the baby universe tails should dominate, leading again to non-physical results. Only in the range such that r is large enough to not be contaminated by the short scale artifacts, but not so large as to be sensitive to the baby universe tails, should the correct behavior emerge. In the continuum limit, the long distance artifacts should vanish.

In the plots of the correlators, the physical regime appears to be the fall off towards a constant. This behavior is seen for all ensembles and curvature definitions except for the simplex curvature with the coarest lattice spacing. At shorter distances, the correlators do not exhibit universal behavior, and can be negative or positive, and have a dip or no dip, depending on the discretization choice for the curvature and on the lattice spacing.

Volume	β	rmin	rmax	a	P	b	$\chi^2/d.o.f.$
32k	0	9	13	$4.13(961) \times 10^{15}$	$-12.6(11)$	$-7.04(27) \times 10^3$	1.28×10^{-3}
16k	0	8	12	$5.0(72) \times 10^{12}$	$-9.7(7)$	$-8.18(42) \times 10^3$	1.02×10^{-1}
8k	0	8	18	$7.7(293) \times 10^{13}$	$-11.3(18)$	$-9.69(39) \times 10^3$	3.16×10^{-1}
4k	0	7	11	$7.3(136) \times 10^{11}$	$-9.30(98)$	$-1.10(55) \times 10^4$	1.09×10^{-2}
4k	1.5	7	18	$2.4(50) \times 10^{13}$	$-11.1(11)$	$-1.44(05) \times 10^4$	1.23×10^{0}
8k	-0.8	7	12	$1.5(55) \times 10^{12}$	$-10.4(19)$	$-8.23(27) \times 10^3$	2.95×10^{-2}

Table 3: The fit results in the universal regime to a power law for the triangle discretization.

Volume	β	rmin	rmax	a	P	b	$\chi^2/d.o.f.$
32k	0	22	44	$4.05(773) \times 10^{14}$	$-8.39(63)$	$-4.87(11) \times 10^3$	2.13×10^{-1}
16k	0	20	38	$1.26(339) \times 10^{15}$	$-9.01(89)$	$-5.074(121) \times 10^3$	4.38×10^{-1}
8k	0	19	32	$3.3(204) \times 10^{14}$	$-8.8(19)$	$-5.06(15) \times 10^3$	1.80×10^{-1}
4k	0	16	29	$1.30(500) \times 10^{14}$	$-8.9(14)$	$-5.92(20) \times 10^3$	5.81×10^{-1}
8k	-0.8	43	58	$1.0(217) \times 10^{28}$	$-15.3(47)$	$-1.780(93) \times 10^3$	7.30×10^{-1}

Table 4: The fit results in the universal regime to a power law for the simplex discretization.

Following de Baker and Smit [40], we explore a power law fit,

$$f(x) = ax^P + b \tag{35}$$

to our data in the "universal" regime. The fits for all ensembles except the 4k $\beta = 1.5$ ensemble in the simplex discretization are given in the Tables (3) and (4) below. Plots showing the fits to the correlators are shown in Figures 37-47.

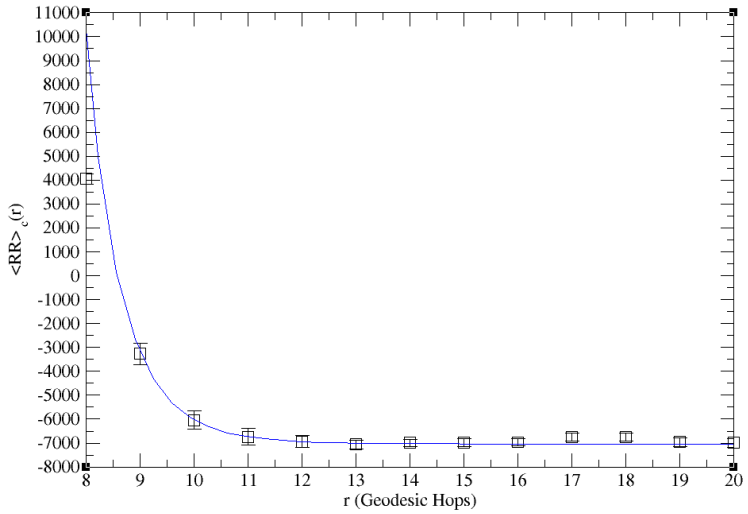

Figure 37: The fit in the universal regime to the 32k $\beta = 0$ ensemble in the triangle discretization. The fit is done in the range [9,13]

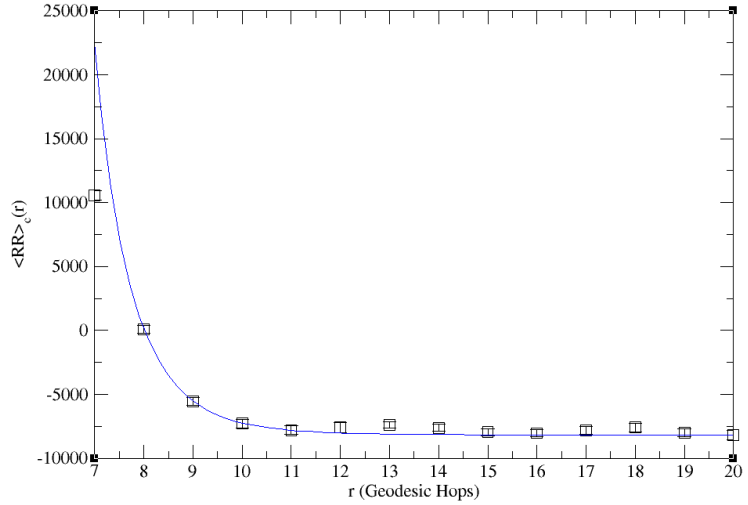

Figure 38: The fit in the universal regime to the 16k $\beta = 0$ ensemble in the triangle discretization. The fit is done in the range [8,12]

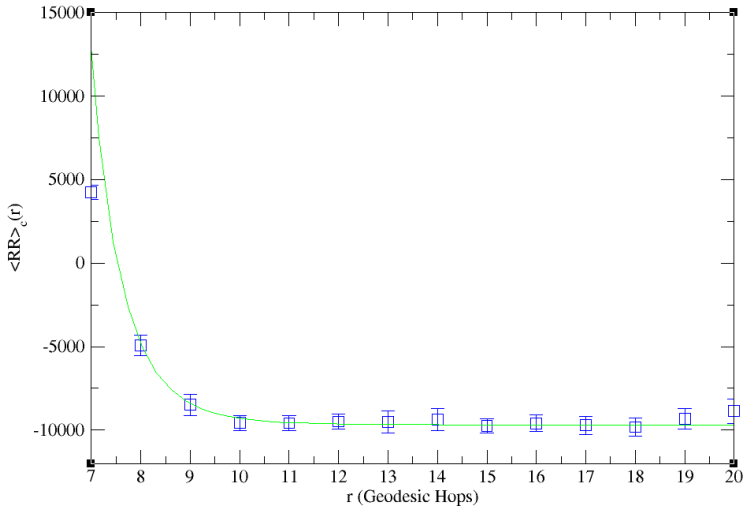

Figure 39: The fit in the universal regime to the 8k $\beta = 0$ ensemble in the triangle discretization. The fit is done in the range [8,18]

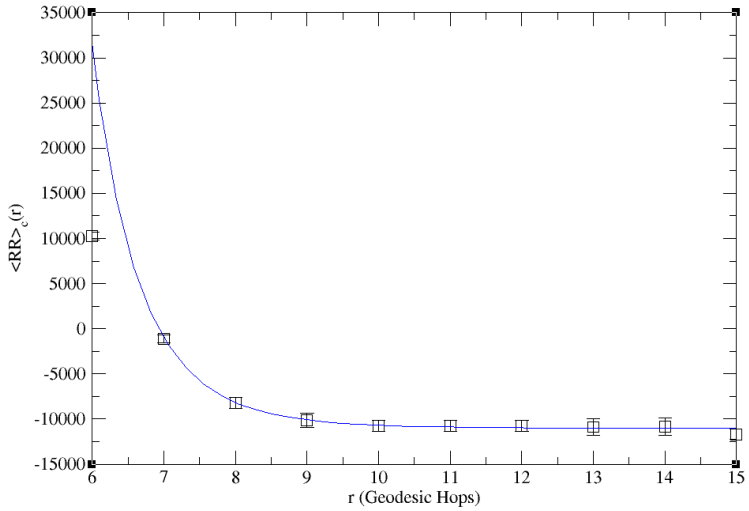

Figure 40: The fit in the universal regime to the 4k $\beta = 0$ ensemble in the triangle discretization. The fit is done in the range [7,11]

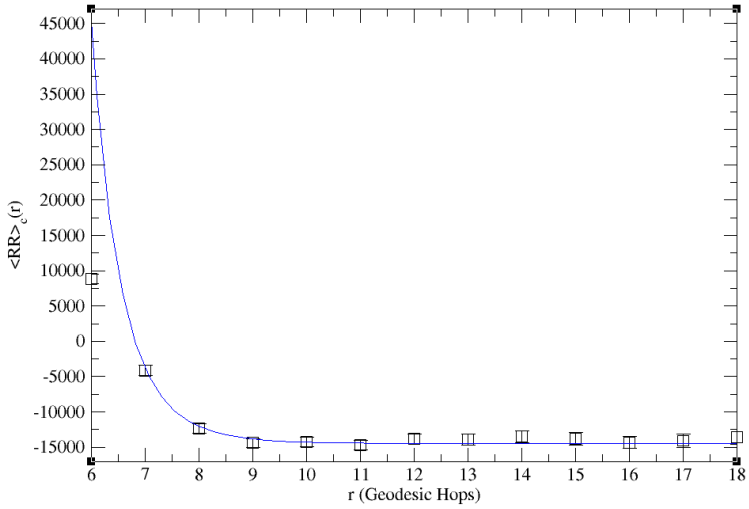

Figure 41: The fit in the universal regime to the 4k $\beta = 1.5$ ensemble in the triangle discretization. The fit is done in the range [7,18]

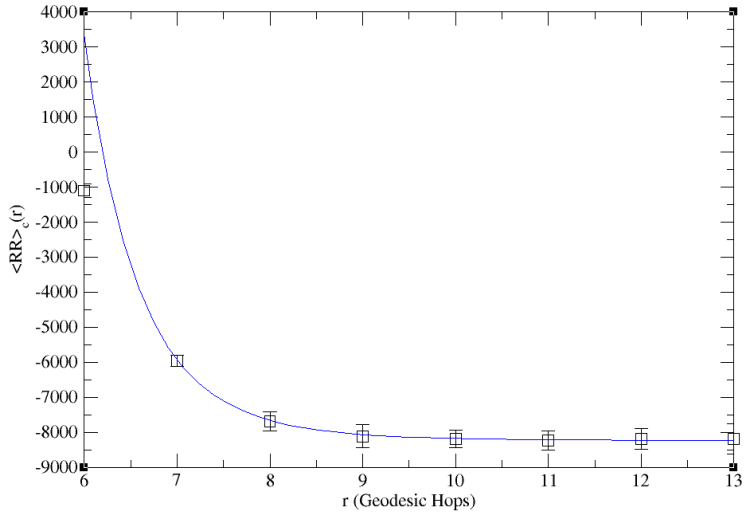

Figure 42: The fit in the universal regime to the 8k $\beta = -0.8$ ensemble in the triangle discretization. The fit is done in the range [7,12]

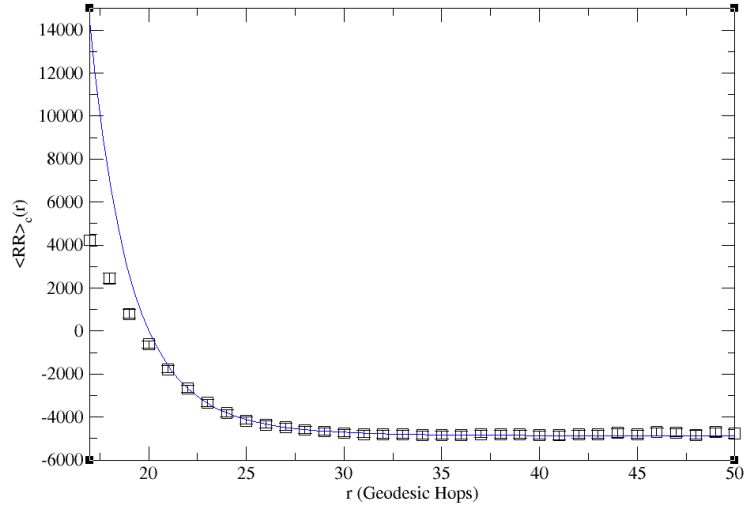

Figure 43: The fit in the universal regime to the 32k $\beta = 0$ ensemble in the simplex discretization. The fit is done in the range [22,44]

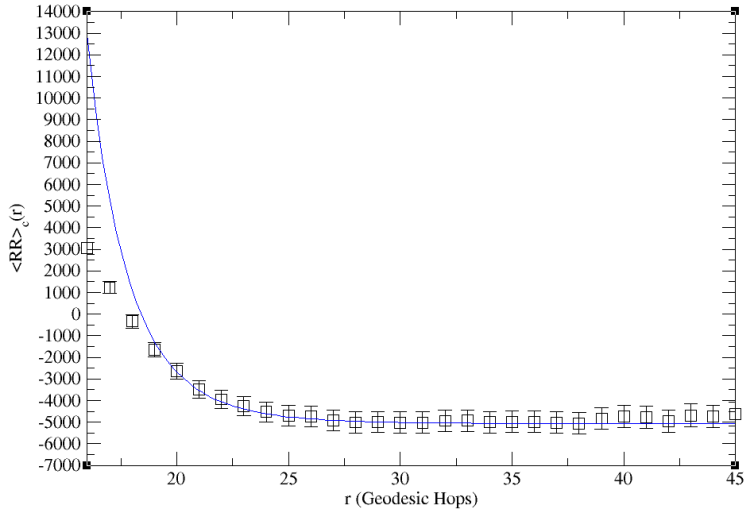

Figure 44: The fit in the universal regime to the 16k $\beta = 0$ ensemble in the simplex discretization. The fit is done in the range [20,38]

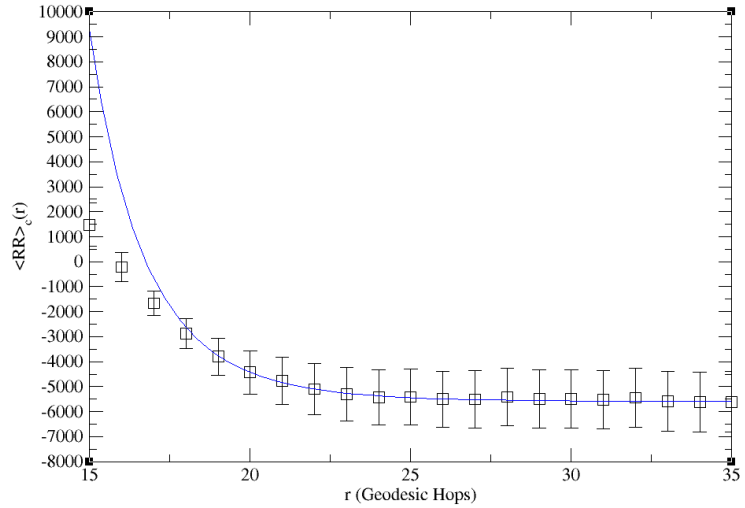

Figure 45: The fit in the universal regime to the 8k $\beta = 0$ ensemble in the simplex discretization. The fit is done in the range [19,32]

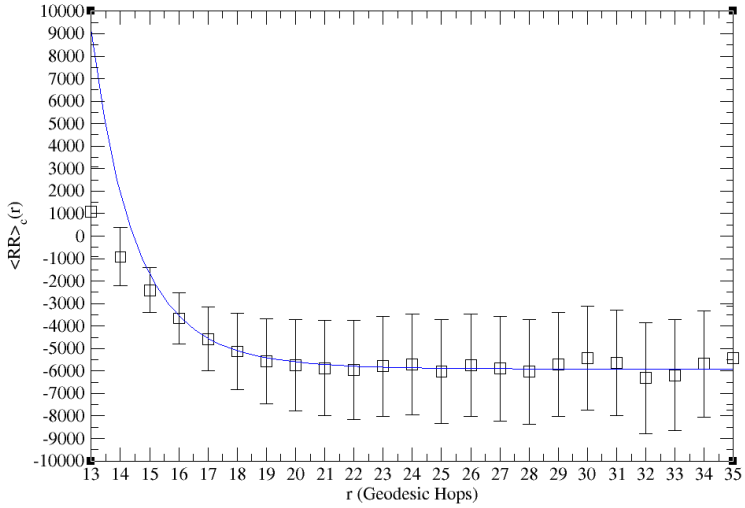

Figure 46: The fit in the universal regime to the 4k $\beta = 0$ ensemble in the simplex discretization. The fit is done in the range [16,29]

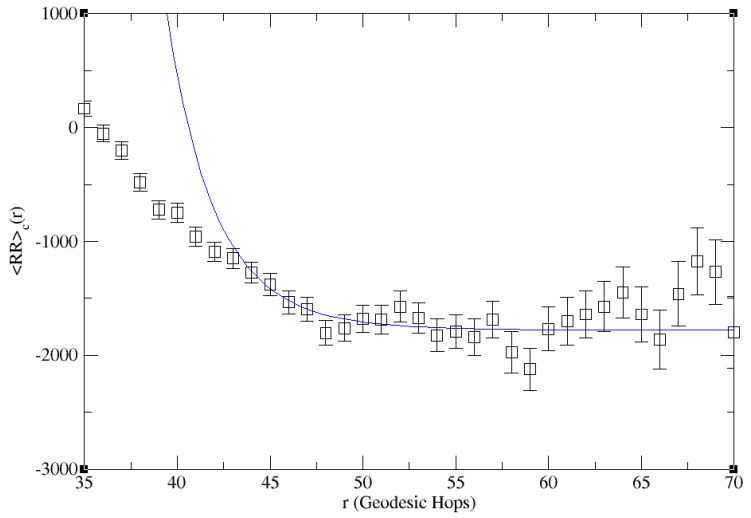

Figure 47: The fit in the universal regime to the 8k $\beta = -0.8$ ensemble in the simplex discretization. The fit is done in the range [43,58]

The smallest value of r in the fit range, r_{min}, is chosen to maximize the number of points that are clearly not a part of the asymptote, while still maintaing a good quality of fit. r_{max} was chosen to include the smallest number of points from the asymptote, while still ensuring that the fit settled on the correct asymptotic value. Fits were tested for many possible fit ranges that satisfied this criteria, until an acceptable fit was found for each ensemble. In general, the fits are excellent, with $\chi^2/d.o.f.$ less than one. One exception is the 4k $\beta = 1.5$ ensemble in the triangle discretization, where the $\chi^2/d.o.f.$ was slightly greater than one.

The 8k $\beta = -0.8$ ensemble in the simplex discretization also appears anomalous. Although the $\chi^2/d.o.f.$ indicates the fit is a good one, the plot in figure 47 shows that this may be misleading. That ensemble's asymptote has a great deal more variance than the others, and it is difficult to identify where the asymptotic behavior begins. Many fits were done across numerous ranges, and a number of candidates were viable for fits to this region. It is difficult to say that this is the best possible fit that correctly accounts for errors in the fit and systematic errors, and this may be the cause of the discrepancy.

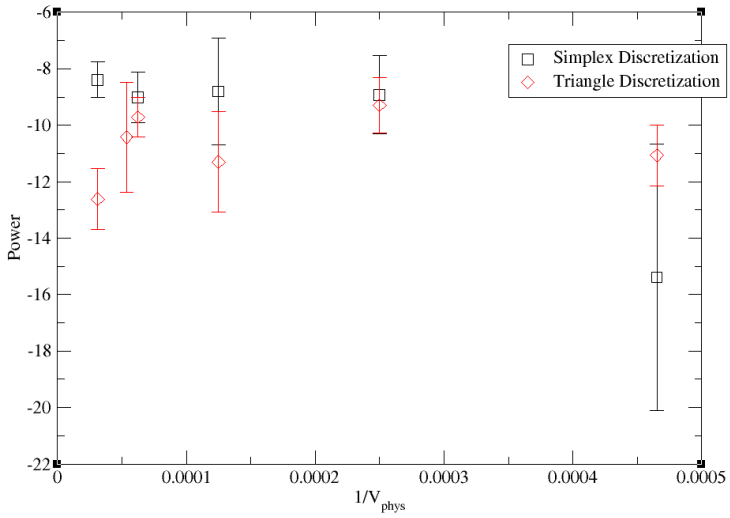

Figure 48: The power of the power law for both the simplex and triangle discretizations.

It remains to determine the power of the power law decay in the infinite volume, continuum limit. The results for the two approaches are plotted together in Figure 48. The two approaches agree, within errors, except for the 32k $\beta = 0$ ensemble. This might be explained by the presence of long distance discretization effects coming from diffeomorphism breaking. When the regulator breaks a symmetry, it is necessary to take the continuum limit before the long distance light modes are properly described. The 32k $\beta = 0$ ensemble has the largest physical volume, but a relatively coarse lattice spacing, and so would be the most likely to be susceptible to such effects.

With the 32k $\beta = 0$ ensemble excluded, the remaining points are best described by a constant fit. The triangle discretization gives a constant of $-10.03(35)$, and the simplex discretization gives $-9.09(54)$. The two approaches are within about 1 σ of each other. The power in the infinite volume, continuum limit appears to be consistent with -10. We discuss in the next section a possible motivation for expecting this value for the power law.

4.4 Coefficient of the Power Law Decay

We have determined that the correlator in the universal regime is compatible with the form

$$\langle RR \rangle_c (r) \sim \frac{A}{r^{10}} + B \tag{36}$$

where B is the asymptote, and A is a dimensionful constant. As curvature has a mass dimension of 2, the correlator has mass dimension of 4, and so A must have dimension -6. The only available quantity in flat space, pure gravity with this dimensionality is G^3, and so

$$A = \alpha c_1 \, G^3 \tag{37}$$

where αc_1 parameterizes the loop factors and other low energy constants in the effective theory of gravity at low energies. In principle, we could get this constant from the fits in the previous section, but the coefficient has very large errors. Instead, we do a volume integral to extract it. We assume that the shift is unphysical, and we will neglect it by adding a constant to the correlator so that the asymptote is set to zero. Thus we have

$$\int d^4x \frac{\alpha c_1 G^3}{r^{10}} = \alpha c_1 G^3 \int_{\ell_{min}}^{\infty} \frac{2\pi^2 r^3 dr}{r^{10}} = \frac{\pi^2}{3} \frac{\alpha c_1 G^3}{\ell_{min}^6} \tag{38}$$

To find this value from the lattice calculation, we need to discretize the volume integration

$$\int d^4x \, \langle RR \rangle_c (r) \to \sum_r \langle RR \rangle_c (r) V(r) \tag{39}$$

where V(r) is the volume at a distance r from the origin. This will be different depending on whether we are dealing with triangles or simplices. For triangles, we have

$$V(r) = \frac{1}{10} \frac{\sqrt{5}}{96} \bar{\mathcal{O}}(r) G^{11}(r) \tag{40}$$

with $\bar{\mathcal{O}}(r)$ the average order of the triangles at a distance r. For simplices, the definition is simpler

$$V(r) = \frac{\sqrt{5}}{96} G^{11}(r) \tag{41}$$

The value of ℓ_{min} is chosen to be the lowest value of r in the universal regime, as determined by the quality of the fits to a power law.

In order to compare the triangle and simplex values for this constant directly, attention must be paid to the different definitions of length. The distance between the centers of two triangles is not the same as the distance between the centers of two simplices. Most of our prior results have been done using simplex distances, so we shall convert the triangle distance to simplex distance.

To get the conversion factor, we compare the location of the peak of the G^{11} distribution of each ensemble for both definitions of distance. The needed factors, listed by β value, are found in Table 45. Note that, contrary to expectation, the factor is different for different β values. Simplices are only required to share a $(d-1)$-subsimplex to be considered neighbors, but triangles have the additional constraint of needing to be members of the same simplex. This added constraint alters how long it takes to traverse the lattice, and therefore how long it takes to reach the peak of the distribution.

With the conversion factor $S(\beta)$ and the relative lattice spacing a_{rel} included, we can find the coefficient αc_1 by equating the two integrated correlators in Eq.(39) and Eq.(40) and isolating $\alpha c_1 G^3$

$$\alpha c_1 G^3 = \frac{3}{\pi^2} (\ell_{min} a_{rel} S(\beta))^6 \sum_{r=\ell_{min}} \langle RR \rangle_c (r) V(r) \tag{42}$$

Volume	β	r_{peak} simplex	r_{peak} triangle	$S(\beta)$
32k	0	20.3-20.8	7.5-8.0	2.71-2.77
16k	0	18.3-18.9	6.7-7.4	2.47-2.82
8k	0	16.3-16.8	6.3-6.9	2.36-2.67
4k	0	14.2-14.7	5.6-6.4	2.22-2.63
4k	1.5	11.6-12.3	5.6-6.5	1.78-2.20
8k	-0.8	30.5-31.5	4.7-5.7	5.35-6.70

Table 5: The fit results in the universal regime to a power law for the simplex discretization.

Note that $S(\beta)$ is just 1 when dealing with the simplex curvature. G is determined by using a dimensionful quantity to set the scale of the lattice, and requires making contact with (semi)classical gravity. Two analyses are currently underway, one involving fluctuations about de Sitter space, and another from studying gravitational interactions between particles via Newton's law. Preliminary results suggest the two approaches roughly agree, but work is still on going.

A plot of $\alpha c_1 G^3$ in the triangle discretization is shown in Figure 49 and in the simplex discretization in Figure 50. The two curvature discretizations are close in magnitude, and appear to trend towards the same answer in the infinite volume, continuum limit. The triangle discretization appears to be non-linear in inverse physical volume $1/V_{phys}$, but not in a simple quadratic way, while still retaining a dependence on lattice spacing. With no theoretical guidance as to what the dependence on volume should be, we adopt the pragmatic approach that we only care about what happens in the infinite volume, continuum limit, and for $\beta = 0$, the approach to large volume becomes linear for the 8k, 16k, and 32k ensembles. We therefore drop both of the ensembles with the smallest physical volume, 4k $\beta = 0$ and 8k $\beta = -0.8$. Though we are left with only two different lattice spacings, we are still able to fit to the function in Eq.(19). This extrapolation is shown in figure 51. The infinite volume, continuum limit of $\alpha c_1 G^3$ for the triangle discretization is $3.8(20) \times 10^{13}$

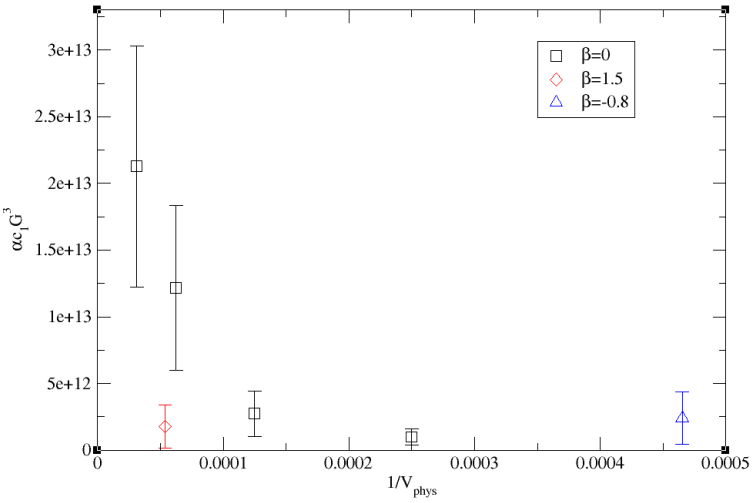

Figure 49: The coefficient $\alpha c_1 G^3$ for the triangle discretization.

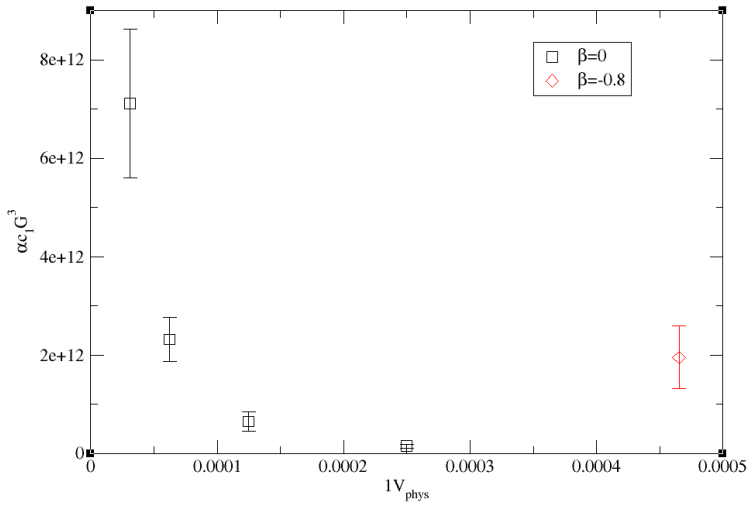

Figure 50: The coefficient $\alpha c_1 G^3$ for the simplex discretization.

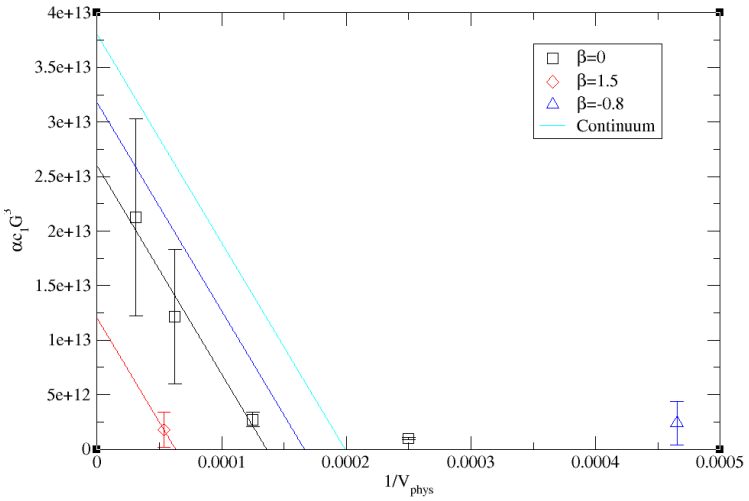

Figure 51: The infinite volume, continuum extrapolation of $\alpha c_1 G^3$ in the triangle discretization. The 4k $\beta = 0$ and 8k $\beta = -0.8$ ensembles were dropped.

The simplex discretization also exhibits a non-quadratic dependence on physical volume, as well as a dependence on lattice spacing. However, if we are forced to omit the 8k $\beta = -0.8$ ensemble, we will be unable to take a continuum limit, since the 4k $\beta = 1.5$ ensemble has already been excluded. We thus retain the 8k $\beta = -0.8$ ensemble, and attempt to fit to a fit function exponential in the inverse physical volume,

$$f(V_{phys}, a) = c_0 + c_1 \exp\left(\frac{c_2}{V_{phys}}\right) + c_3 a^2, \tag{43}$$

where c_i are fit parameters. The extrapolation is shown in Figure 52. The infinite volume, continuum limit of $\alpha c_1 G^3$ in the simplex discretization is $2.61(11) \times 10^{13}$.

Though the fits are poorly constrained due to each only including two different lattice spacings, we find that the two discretization are very close, $3.8(20) \times 10^{13}$ in the triangle discretization, and $2.61(11) \times 10^{13}$ in the simplex discretization. The two results are separated by less than 1 σ, and so we find there to be good agreement. We submit that this value is

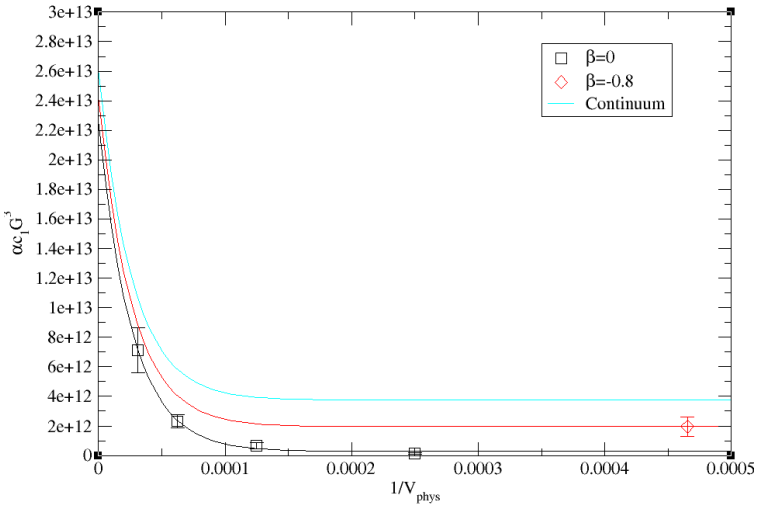

Figure 52: The infinite volume, continuum limit extrapolation of $\alpha c_1 G^3$ in the simplex discretization.

universal regardless of the choice of discretization.

It is clear that $\alpha c_1 G^3$ is a very large coefficient. The simplest explanation for this large coefficient that maintains a connection with the low energy effective theory is that the $\sqrt{g}R^2$ in the effective actiont has a large coefficient. Intriguingly, there exists a theory of inflation, the Starobinsky Model [44], that explains inflation with an R^2 term with a very large coefficient. Since our approach to gravity has no free parameters in the gravity sector, the Starobinsky model cannot be added "by hand" to our approach. The coefficient of the R^2 term is a prediction in our model, allowing us to potentially determine the inflationary potential from first principles with no adjustable parameters. If the predicted coefficient was compatible with observations, it would have serious implications for observational cosmology, allowing us to predict all of the properties of the anisotropies in the cosmic microwave background.

That the coefficient is very large supports our result that the power of the decay in the previous section is -10. The tree-level classical contributions to this correlator begin at $\frac{G}{r^6}$. This term, however, vanishes at tree-level [47]. The next contribution should then begin

at one loop and be proportional to $\frac{G^2}{r^8}$. The preliminary calculations for G that we have conducted suggest that G is $\mathcal{O}(1)$, and so in order to obtain a large coefficient, one of the R^2 terms must come with a large coefficient. These terms first contribute at $\frac{G^3}{r^{10}}$. There are two $\mathcal{O}(R^2)$ terms, R^2 and C^2 (The Weyl Squared term). If the C^2 term comes with a large coefficient, Newton's law would be modified to become repulsive. Repulsive gravity does not appear in our analysis in another on-going study, so the large coefficient must be due to the R^2 term if we are to make contact with the low energy effective theory.

5 Conclusions

The implementation of gravity on the lattice, EDT, has received renewed interest. The introduction and reinterpretation of a non-trivial measure term has lead to a recovery of semi-classical gravity in the appropriate limit, once the free parameter in the measure term is fine-tuned to restore diffeomorphism invariance. We have shown that, in addition to hints that we recover the correct 4-dimensional space-time, that there is evidence for a continuum limit at a non-trivial UV fixed point.

In this work, we've seen that of the dimensionless physical couplings, $\hat{G}$ and $\hat{\Lambda}$ separately are not relevant couplings. Rather, the product $G\Lambda$ is the relevant coupling that is expected to approach a fixed point in the UV. We argue that the running of β is unphysical, and that β is the free parameter in the action that must be tuned to restore diffeomorphism invariance. This unphysical running of β introduces an unphysical running into $\hat{\Lambda}$ that must be subtracted. To achieve this, we determine a subtracted β as follows: we calculate $G\Lambda$ along lines of fixed β with varied κ_2, and look for a curve where $G\Lambda$ has a zero and a zero derivative at the same point. We find no barrier to finding this value of β for any lattice volume. If $G\Lambda$ is the only relevant coupling after accounting for symmetry breaking by the lattice regulator, then we need only input a single dimensionful parameter to set the scale, and then all other quantities become predictions.

We examined the two point curvature correlation function using two different curvature discretizations. The simplest attempt to find the correlation function for curvature suffers from an overcounting of geometry, since the distance between two points is a geometric object. The disconnected part of the correlator must be subtracted out so that the correct correlators are obtained. We find that there is a universal power law decay with an infinite volume, continuum limit, and find it to be consistent between two different discretizations of the curvature.

Upon integrating the curvature correlation functions over volume, we also obtain the coefficient of the power law, which again appears to be independent of whether triangle curvature or simplex curvature is used. The coefficient is found to be much larger than what one would expect from naive power counting arguments in low energy effective theory. It is in principle possible to translate this coefficient into the coupling of the $\sqrt{g}R^2$ term in the low energy effective Lagrangian for gravity in the infinte volume flat-space limit. If this result holds up, it would provide a quantum gravitational origin for inflation vis a vie the Starobinsky model, but with no free parameters. This would be a highly predictive, and thereby falsifiable, theory of quantum gravity.

Much work remains. To better control the infinite volume and continuum extrapolations, lattices at finer lattice spacings and larger lattice volumes are needed. Matter fields also need to be added to examine what effect they have on the phase diagram and the quantities studied here. Quenched scalar fields have already been implemented, but back reactions on the geometry must still be included. Work on this is in progress. An approach to implementing fermions on dynamical triangulations has recently been introduced. Work is on going to include the back reaction of fermions on the geometry as well. These matter effects must ultimately be included if we are to compare our predictions with observational cosmology. We also need the one loop coefficient from the low energy effective theory to match our calculations to experiment, and this is also in progress.

References

[1] M. H. Goroff and A. Sagnotti, Nucl.Phys. **B266**, 709 (1986).

[2] G. 't Hooft and M. Veltman, Annales Poincare Phys.Theor. **A20**, 69 (1974).

[3] S. Weinberg, in *Sources and detection of dark matter and dark energy in the universe. Proceedings, 4th International Symposium, DM 2000, Marina del Rey, USA, February 23-25, 2000* (2000), pp. 18–26, astro-ph/0005265, URL-http://www.slac.stanford.edu/spires/find/books/www?cl=QB461:I57:2000.

[4] S. Weinberg, in General Relativity: An Einstein Centenary Survey(1980), pp. 790–831.

[5] T. Regge, *General Relativity without Coordinates*, Nuovo Cimento,XIX, 3, 559 (1961)

[6] M. E. Agishtein and A. A. Migdal, Mod. Phys. Lett.A7, 1039 (1992).

[7] J. Ambjorn and J. Jurkiewicz, Phys.Lett.B278, 42 (1992), revision of NBI-HE-91-47.

[8] J. Ambjorn, Grav. Cosmol.8, 144 (2002).

[9] B. V. de Bakker and J. Smit, Nucl. Phys.B439, 239 (1995), hep-lat/9407014.

[10] J. Ambjorn and J. Jurkiewicz, Nucl. Phys.B451, 643 (1995), hep-th/9503006.

[11] S. Catterall, J. B. Kogut, and R. Renken, Phys. Lett.B328, 277 (1994), hep-lat/9401026.

[12] H. S. Egawa, T. Hotta, T. Izubuchi, N. Tsuda, and T. Yukawa, Prog. Theor. Phys.97, 539(1997), hep-lat/9611028.

[13] P. Bialas, Z. Burda, A. Krzywicki, and B. Petersson, Nucl.Phys.B472, 293 (1996), hep-lat/9601024.

[14] B. V. de Bakker, Phys.Lett.B389, 238 (1996), hep-lat/9603024.

[15] B. Bruegmann and E. Marinari, Phys.Rev.Lett.70, 1908 (1993), hep-lat/9210002.

[16] S. Bilke, Z. Burda, A. Krzywicki, B. Petersson, J. Tabaczek, et al., Phys.Lett.B432, 279(1998), hep-lat/9804011.

[17] J. Ambjorn, L. Glaser, A. Goerlich, and J. Jurkiewicz, JHEP1310, 100 (2013), 1307.2270.

[18] D. Coumbe and J. Laiho, JHEP04, 028 (2015), 1401.3299.

[19] J. Ambjorn, J. Jurkiewicz, and R. Loll, Phys. Rev. Lett.93, 131301 (2004), hep-th/0404156.

[20] J. Ambjorn, J. Jurkiewicz, and R. Loll, Phys. Rev.D72, 064014 (2005), hep-th/0505154.

[21] M. Gross and S. Varsted, Nucl. Phys.B378, 367 (1992).

[22] S. Bilke and G. Thorleifsson, Phys.Rev.D59, 124008 (1999), hep-lat/9810049.

[23] J. Smit, JHEP08, 016 (2013), [Erratum: JHEP09,048(2015)], 1304.6339.

[24] C. Bernard, Phys. Rev.D71, 094020 (2005), hep-lat/0412030.

[25] J. Ambjorn, A. Gorlich, J. Jurkiewicz, and R. Loll, Phys. Rev.D78, 063544 (2008),arXiv:0807.4481.

[26] T. P. Peixoto, figshare (2014), URL http://figshare.com/articles/graph_tool/1164194.

[27] J. Ambjorn (Private communication).

[28] R. L. Renken, S. M. Catterall, and J. B. Kogut, Nucl. Phys.B523, 553 (1998), hep-lat/9712011.

[29] G. Thorleifsson, P. Bialas, and B. Petersson, Nucl. Phys.B550, 465 (1999), hep-lat/9812022.

[30] D. Benedetti and R. Gurau, Nucl. Phys.B855, 420 (2012), 1108.5389.

[31] J. Ambjorn, A. Gorlich, J. Jurkiewicz, and R. Loll, Phys.Rev.Lett.100, 091304 (2008),arXiv:0712.2485.

[32] D. N. Coumbe and J. Jurkiewicz, JHEP03, 151 (2015), 1411.7712.

[33] J. Ambjorn, J. Jurkiewicz, and R. Loll, Phys. Rev. Lett.95, 171301 (2005), hep-th/0505113.

[34] O. Lauscher and M. Reuter, JHEP0510, 050 (2005), hep-th/0508202.

[35] G. Calcagni, D. Oriti, and J. Thrigen, Class. Quant. Grav.31, 135014 (2014), 1311.3340.

[36] S. Jordan and R. Loll, Phys.Lett.B724, 155 (2013), 1305.4582.

[37] T. Banks (2010), arXiv:1007.4001.

[38] E. Akkermans, G. V. Dunne, and A. Teplyaev, Phys.Rev.Lett.105, 230407 (2010),arXiv:1010.1148.

[39] S. Carlip and D. Grumiller, Phys. Rev.D84, 084029 (2011), 1108.4686.

[40] de Bakker, B. V., & Smit, J. (1995). Two Point functions in 4-d Dynamical Triangulation. Nuclear Physics B,454(B), 343-356. DOI: 10.1016/0550-3213(95)00381-2 arXiv:hep-lat/9503004

[41] P. Bialas, Phys. Lett. B373 (1996) 289.P. Bialas, Nucl. Phys. Proc. Suppl. 53 (1997) 739. hep-lat/9608029

[42] Ambjørn, P. Bialas, and J. Jurkiewicz, JHEP 9902 (1999) 005.

[43] H. W. Hamber, Phys. Rev.D92, 064017 (2015), arXiv:1506.07795 [hep-th]

[44] A. A. Starobinsky, Phys. Lett. B91, 99 (1980) [Phys. Lett.91B, 99 (1980)] [Adv. Ser. Astrophys.Cosmol.3, 130 (1987)]

[45] Raghav G. Jha, Jack Laiho, Judah Unmuth-Yockey arXiv:1810.09946 [hep-lat]

[46] Simon Catterall, Jack Laiho, Judah Unmuth-Yockey arXiv:1810.10626 [hep-lat]

[47] G. Modanese, Phys. Lett. B288 (1992) 69; Riv. Nuovo Cimento17 (1994) 1.

6 Curriculum Vitae

Scott Bassler

132J Remington Avenue Syracuse NY, 13210

sdbassle@syr.edu | 1-(732)-567-7677

Education

- **Ph. D. Theoretical Physics** 2013-2019

  Syracuse University, Syracuse NY, 13210 GPA: 3.73

- **B.S. Applied Physics** 2009-2013

  Stockton University, Pomona NJ, 08240 GPA: 3.95

Experience

- **Instructor: Astronomy 101, Astronomy 104** 2014-2016

  Syracuse University

  Responsibilities: Give lectures, create and grade homework and exams.

- **Head TA: Astronomy 101, Astronomy 104** 2014-2018

  Syracuse University

  Responsibilities: Organize TAs, choose and modify labs each week, set up equipment, create grading rubric, run lab sections.

- **TA: Astronomy 101, Physics 221** 2013-2014

  Syracuse University

  Responsibilities: Run lab sections, grade assignments, give student feedback.

- **TA: Physics I and II Laboratory** 2012-2013

  Stockton University

  Responsibilities: Assist the professor in the lab by answering student questions and grading assignments.

- **Grader: Physics I and II** 2010-2013

  Stockton University

  Responsibilities: Grading assignments, responding to student concerns, and giving feedback to the professor.

Additional Employment

- **Substitute Teacher** 2010-2012

  Woodbury Jr. Sr. High School, Woodbury NJ, 08096

Awards

- **Outstanding TA Award** 2016

  Awarded to Teaching Assistants at Syracuse University for their distinguished contributions to the university by demonstrating excelling in significant instructional capacities.

- **Yitzhak Sharon Book Award** 2012

  Awarded by Dr. Yitzhak at Stockton University to a full-time physics undergraduate for character and achievement.

- **Paul Saraduke Memorial Physics Award** 2011

  Awarded by Stockton Faculty to a physics student displaying excellence in undergraduate physics.

- **Stockton Presidential Scholarship** 2009

  Awarded to incoming students with high standardized test results and class ranks.

Publications and Talks

- **Talk:** Curvature Correlators in Lattice Quantum Gravity

  S. Bassler, J. Laiho, J. Unmuth-Yockey, R Jha

  Lattice 2018

- **Publication:** Lattice Quantum Gravity and Asymptotic Safety

  J. Laiho, S. Bassler, D. Coumbe, D. Du, and J. T. Neelakanta

  Phys. Rev. D 96, 064015 – Published 12 September 2017